Electronic Supplementary Material (ESI) for Journal of Materials Chemistry A.

— Supplementary Information —

Defect Chemistry and Doping of BiCuSeO

Michael Y. Toriyama,[*,†] Jiaxing Qu,[‡] G. Jeffrey Snyder,[†] and Prashun Gorai[*,¶]

†*Materials Science and Engineering, Northwestern University, Evanston, IL 60208, USA.*

‡*Mechanical Engineering, University of Illinois at Urbana-Champaign, Urbana, IL 61801.*

¶*Metallurgical and Materials Engineeering, Colorado School of Mines, Golden, CO 80401, USA.*

E-mail: MichaelToriyama2024@u.northwestern.edu; pgorai@mines.edu

Pristine and Interstitial Structures

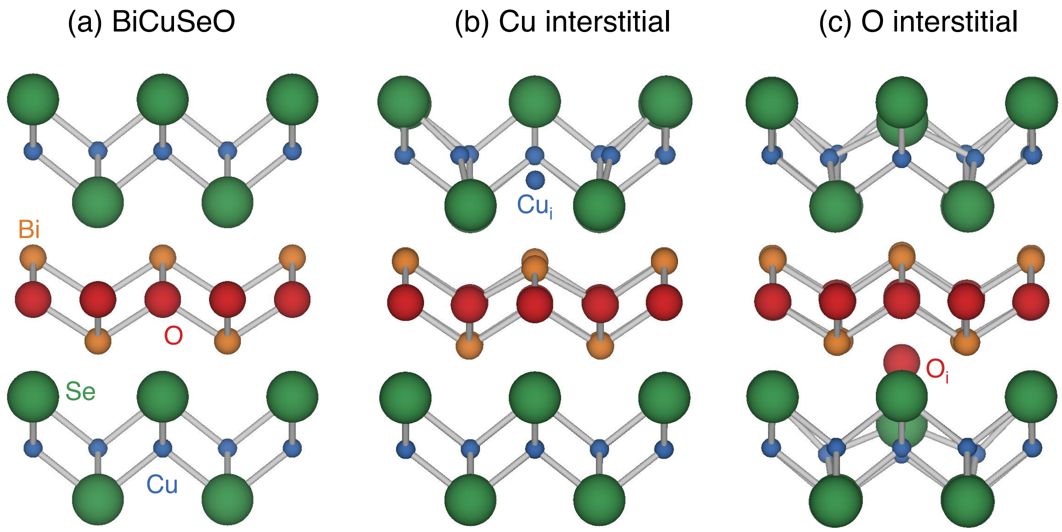

Figure S1: (a) Crystal structure of BiCuSeO, (b) Structure of copper interstitial (Cu_i^{+1}), and (c) Structure of oxygen interstitial (O_i^0).

Calculated Lattice Parameters

Method	a (Å)	c (Å)	a Error (%)	c Error (%)
PBE + U	3.949	9.062	0.52	1.49
vdW + U	3.926	8.927	0.08	0.02
Experiment [1]	3.929	8.929		

Table S1: Lattice constants calculated using different functionals and compared to experimental values. [1] The experimental lattice constants are better reproduced with the van der Waals-corrected functional with Hubbard U correction (vdW+U).

Electronic Structure of BiCuSeO

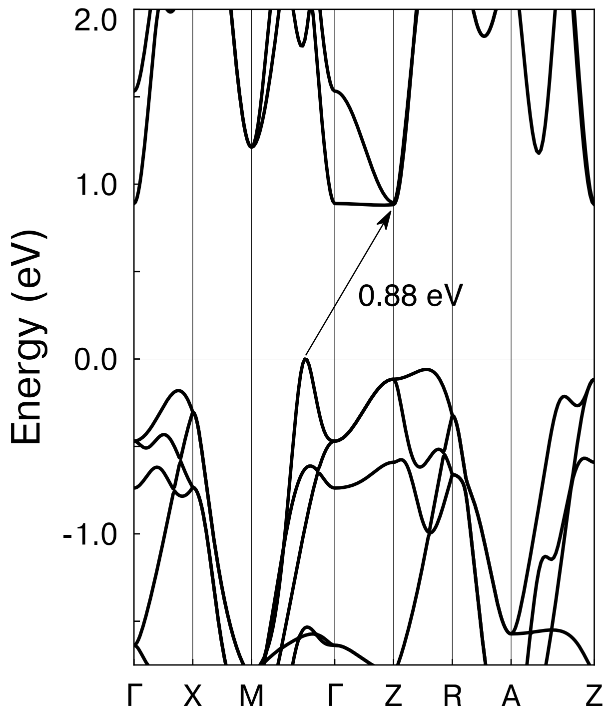

Figure S2: Computed electronic band structure of BiCuSeO along the special k-point paths of the Brillouin zone. The band edge positions are rigidly shifted to according to GW and spin-orbit coupling calculations.

Elemental Reference Chemical Potentials

Element	μ^0 (eV)
Bi	-4.42
Cu	-1.65
Se	-3.63
O	-4.76
Li	-1.64
Zn	-0.80
Mg	-1.00
Ca	-1.60
Sr	-1.15
Ba	-1.34
Al	-2.81
Ga	-2.30
In	-2.27
Tl	-2.35
Si	-4.74
Ge	-4.07
Sn	-3.65
Pb	-3.79
Sc	-4.49
Y	-4.81
Ti	-5.39
Zr	-5.97
Hf	-7.51
F	-1.52
Cl	-1.73
Br	-1.74
I	-1.67

Table S2: Elemental reference chemical potentials μ^0, fitted to experimental formation enthalpies.[2,3] GGA+U functional is used to calculate the total energy of the compounds used in the fitting.

Phase Equilibria of BiCuSeO

Equilibrium Phases	$\Delta\mu_{Bi}$	$\Delta\mu_{Cu}$	$\Delta\mu_{O}$	$\Delta\mu_{Se}$	$p - n$ (cm^{-3})
Se, Cu_3Se_2, Bi_2Se_3	-0.378	-0.62	-1.923	0.0	7.36×10^{19}
Se, Bi_2O_2Se, Bi_2O_3	-0.602	-0.708	-1.61	0.0	1.26×10^{20}
Se, Bi_2O_2Se, Bi_2Se_3	-0.378	-0.708	-1.835	0.0	1.25×10^{20}
Se, Cu_3Se_2, Bi_2O_3	-0.865	-0.62	-1.435	0.0	7.48×10^{19}
Cu_2O, Cu_3Se_2, Bi_2O_3	-0.603	-0.445	-1.61	-0.262	2.6×10^{19}
Cu_2Se, Cu_2O, Cu_3Se_2	-0.285	-0.318	-1.864	-0.453	1.13×10^{19}
Bi, Cu_2O, Bi_2O_3	0.0	-0.244	-2.012	-0.664	5.61×10^{18}
Bi, Cu_2Se, Cu_2O	0.0	-0.223	-2.054	-0.643	5.11×10^{18}
Bi, Cu_2Se, Cu_3Se_2	0.0	-0.318	-2.149	-0.453	1.1×10^{19}
Bi, Cu_3Se_2, Bi_2Se_3	0.0	-0.452	-2.216	-0.252	2.33×10^{19}
Bi, Bi_2O_2Se, Bi_2O_3	0.0	-0.507	-2.012	-0.402	3.44×10^{19}
Bi, Bi_2O_2Se, Bi_2Se_3	0.0	-0.582	-2.087	-0.252	5.4×10^{19}

Table S3: Chemical potentials $\Delta\mu_i$ (in eV) in all phase regions of the quaternary Bi-Cu-Se-O phase space that are in equilibrium with BiCuSeO. The corresponding charge carrier concentration in each phase region, as determined by charge neutrality at the typical synthesis temperature of 973 K, is listed.

Native Defects in BiCuSeO

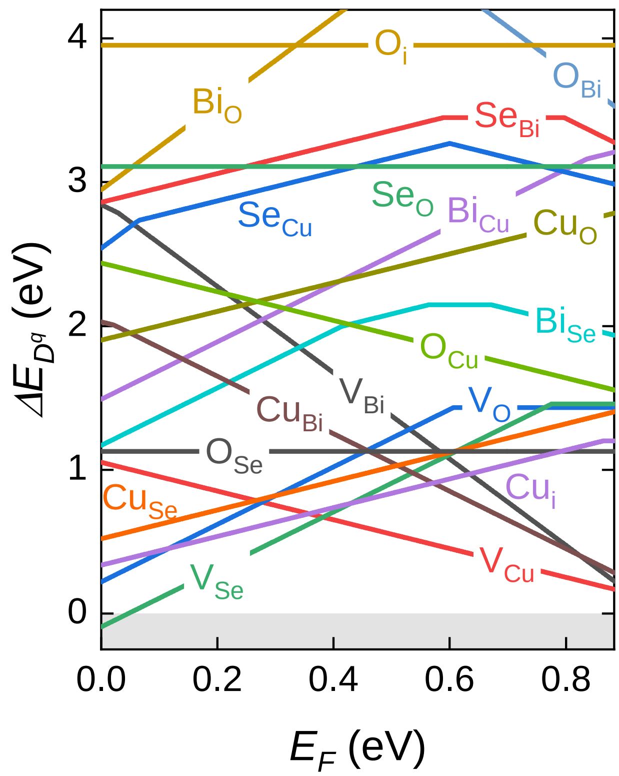

Figure S3: Formation energy (ΔE_{D^q}) as a function of Fermi energy (E_F) of all native defects in BiCuSeO under the most Cu-rich condition where BiCuSeO is in equilibrium with Bi, Cu_2Se, and Cu_2O.

Group-2 Doping: Mg, Ca, Sr, Ba

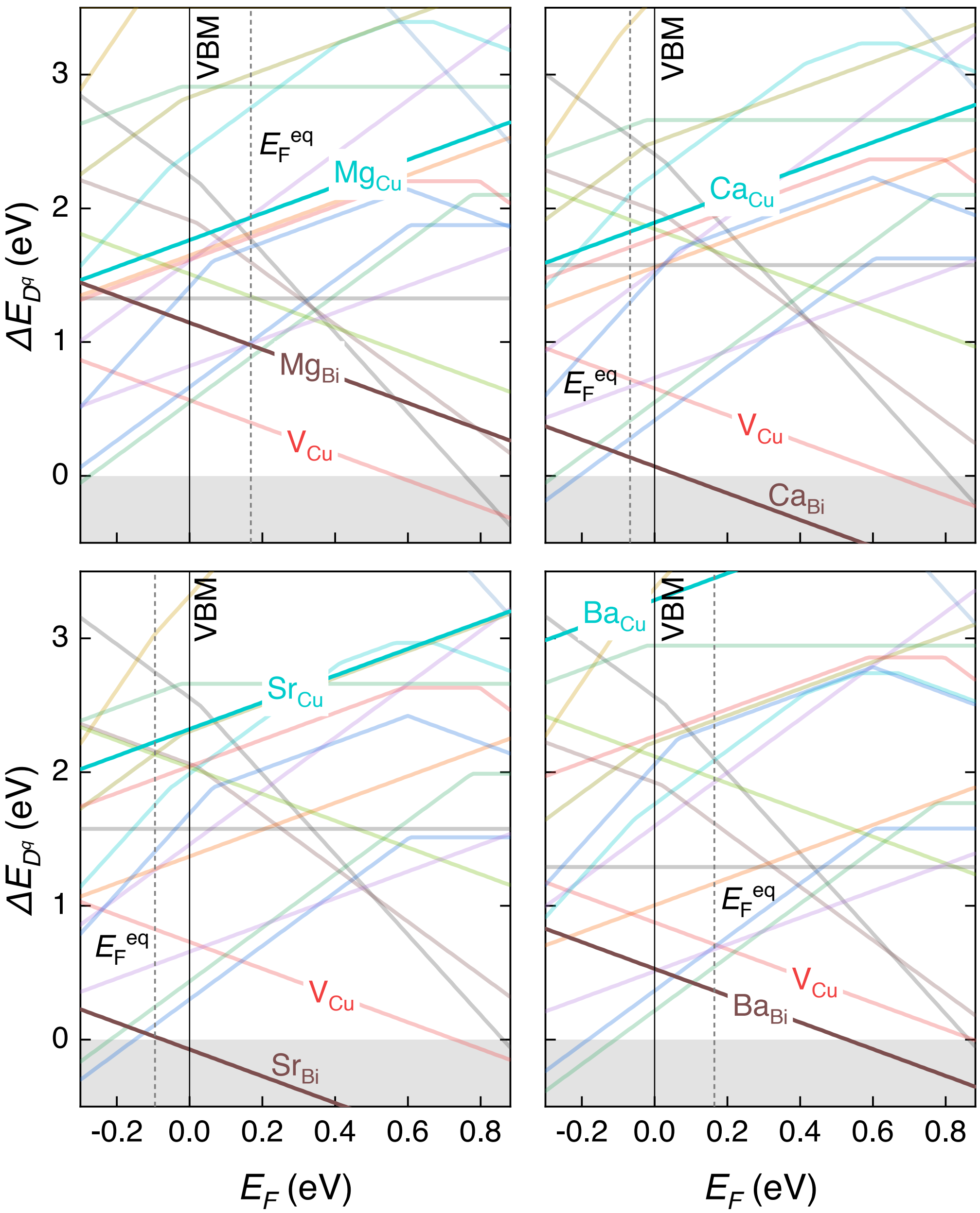

Figure S4: Formation energy of defects associated with (a) Mg, (b) Ca, (c) Sr, and (d) Ba doping under the most Cu-poor and dopant-rich conditions i.e., phase regions that yield the highest hole concentrations. BiCuSeO is in equilibrium with the following phases: (a) Se, MgO, Bi_2O_2Se, and Bi_2O_3, (b) Se, CaO, Cu_3Se_2, and $CaSeO_3$, (c) $SrSeO_3$, SrSe, $Bi_2O_5Sr_2$, and Cu_3Se_2, and (d) $BaCu_2Se_2$, $BaSeO_3$, Cu_3Se_2, and $Ba_2Bi_4O_8$. Native defects of BiCuSeO (Figure 2 in the main text) are shown in lighter colors. The valence band maximum (VBM) is shown as the vertical solid line at $E_F = 0$. The equilibrium Fermi energy (E_F^{eq}) is shown as the dotted vertical line.

Group-17 Doping: F

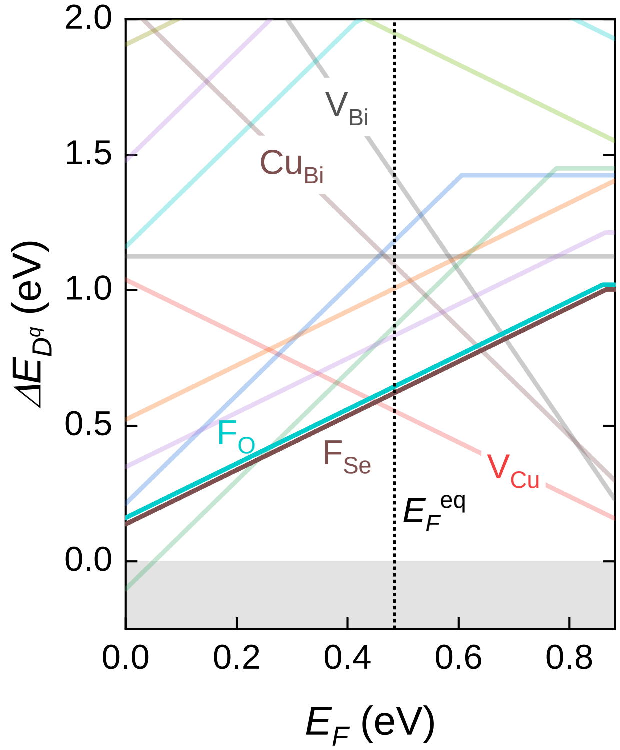

Figure S5: Formation energy of defects associated with F doping under the most Cu-rich condition, where BiCuSeO is in equilibrium with Bi, Cu_2O, Cu_2Se, and BiFO. Native defects of BiCuSeO (Figure 2 in main text) are shown in lighter colors. The equilibrium Fermi energy (E_F^{eq}), as determined by charge neutrality at 973 K, is marked with a dotted vertical line.

Group-1 Doping: Li

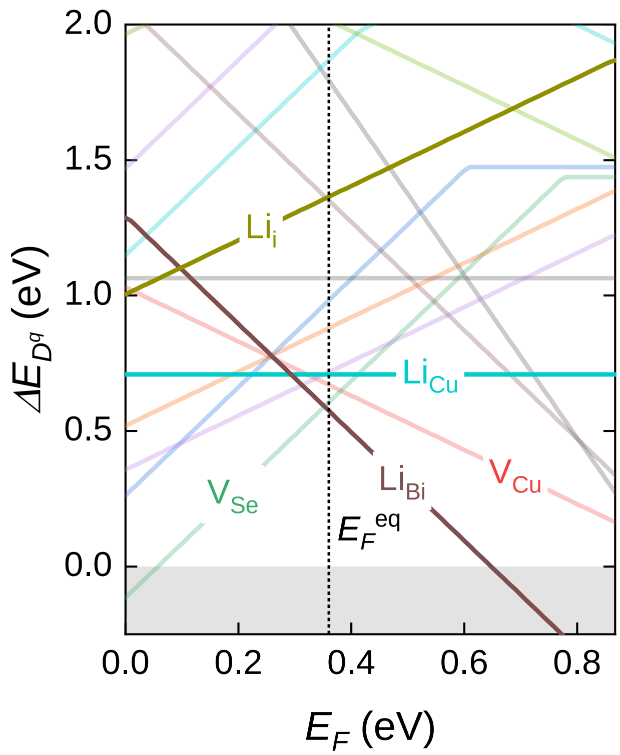

Figure S6: Formation energy of defects associated with Li doping in BiCuSeO under the most Cu-rich condition where BiCuSeO is in equilibrium with Bi, Cu_2O, Bi_2O_3, and $Cu_8Li_8O_8$. Native defects of BiCuSeO (Figure 2 in main text) are shown in lighter colors. The equilibrium Fermi energy (E_F^{eq}), as determined by charge neutrality at 973 K, is marked with a dotted vertical line.

Group-12 Doping: Zn

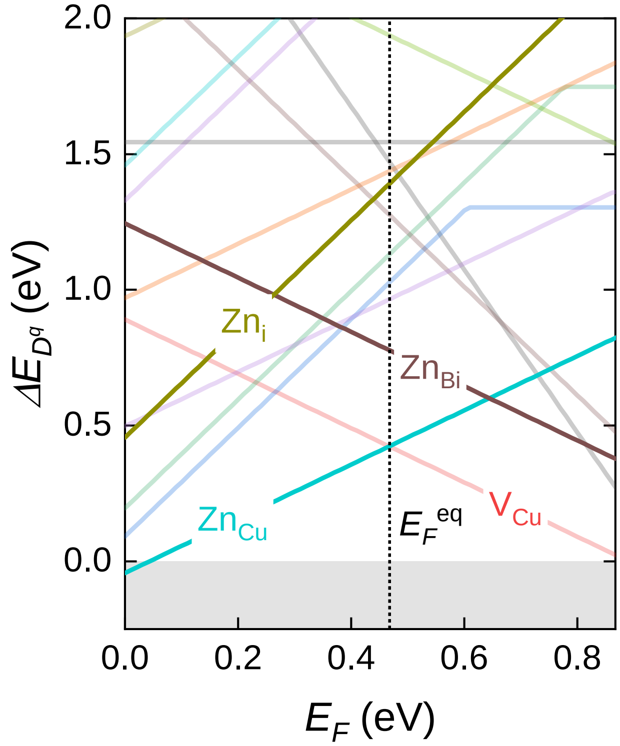

Figure S7: Formation energy of defects associated with Zn doping in BiCuSeO under the thermodynamic conditions where BiCuSeO is in equilibrium with Bi, Cu_3Se_2, ZnSe, and ZnO. Native defects of BiCuSeO (Figure 2 in main text) are shown in lighter colors. The equilibrium Fermi energy (E_F^{eq}), as determined by charge neutrality at 973 K, is marked with a dotted vertical line.

Group-3 Doping: Sc, Y

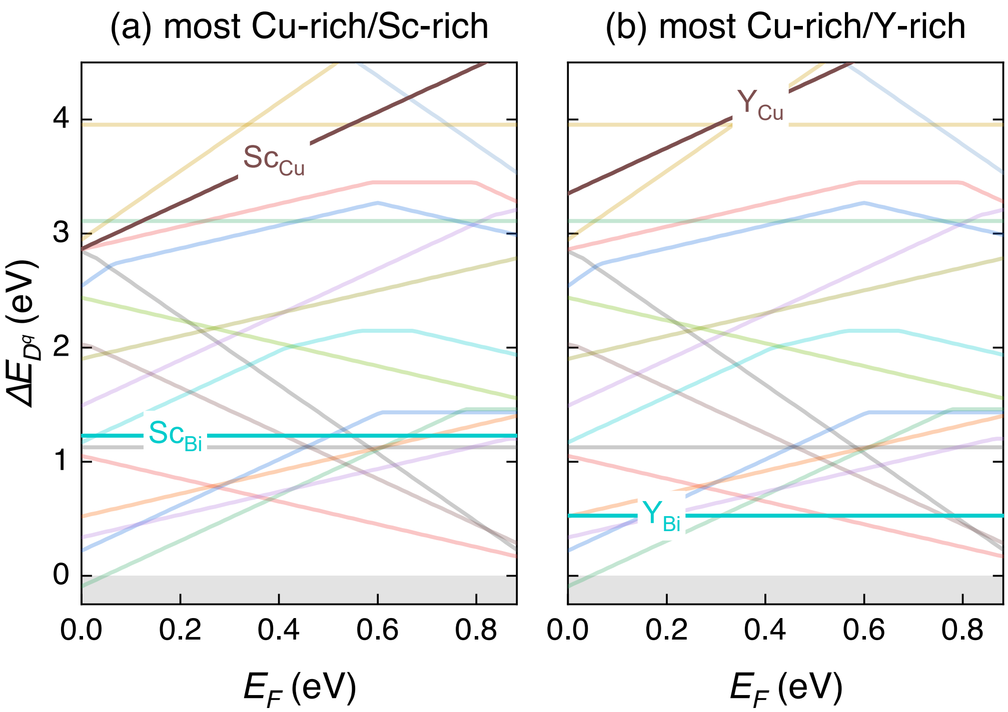

Figure S8: Formation energy of defects associated with (a) Sc, and (b) Y doping in BiCuSeO under the most Cu-rich conditions where BiCuSeO is in equilibrium with (a) Bi, Cu_2Se, Cu_2O, and CuO_2Sc, and (b) Bi, Cu_2Se, Cu_2O, and Y_2O_3. Native defects of BiCuSeO (Figure 2 in main text) are shown in lighter colors. The equilibrium Fermi energy (E_F^{eq}), as determined by charge neutrality at 973 K, is marked with a dotted vertical line.

Group-4 Doping: Ti, Zr, Hf

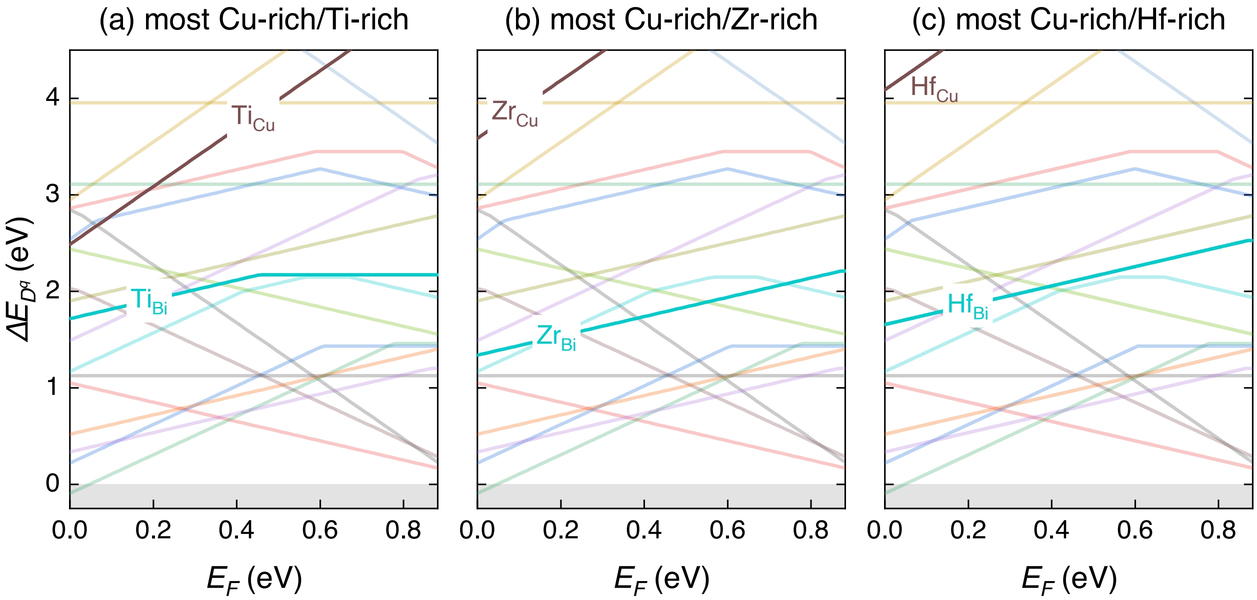

Figure S9: Formation energy of defects associated with (a) Ti, (b) Zr, and (c) Hf doping in BiCuSeO under Cu-rich conditions where BiCuSeO is in equilibrium with (a) Bi, Cu_2Se, Cu_2O, and $Bi_2O_7Ti_2$, (b) Bi, Cu_2Se, Cu_2O, and ZrO_2, and (c) Bi, Cu_2Se, Cu_2O, and HfO_2. Native defects of BiCuSeO (Figure 2 in main text) are shown in lighter colors. The equilibrium Fermi energy (E_F^{eq}), as determined by charge neutrality at 973 K, is marked with a dotted vertical line.

Group-13 Doping: Al, Ga, In, and Tl

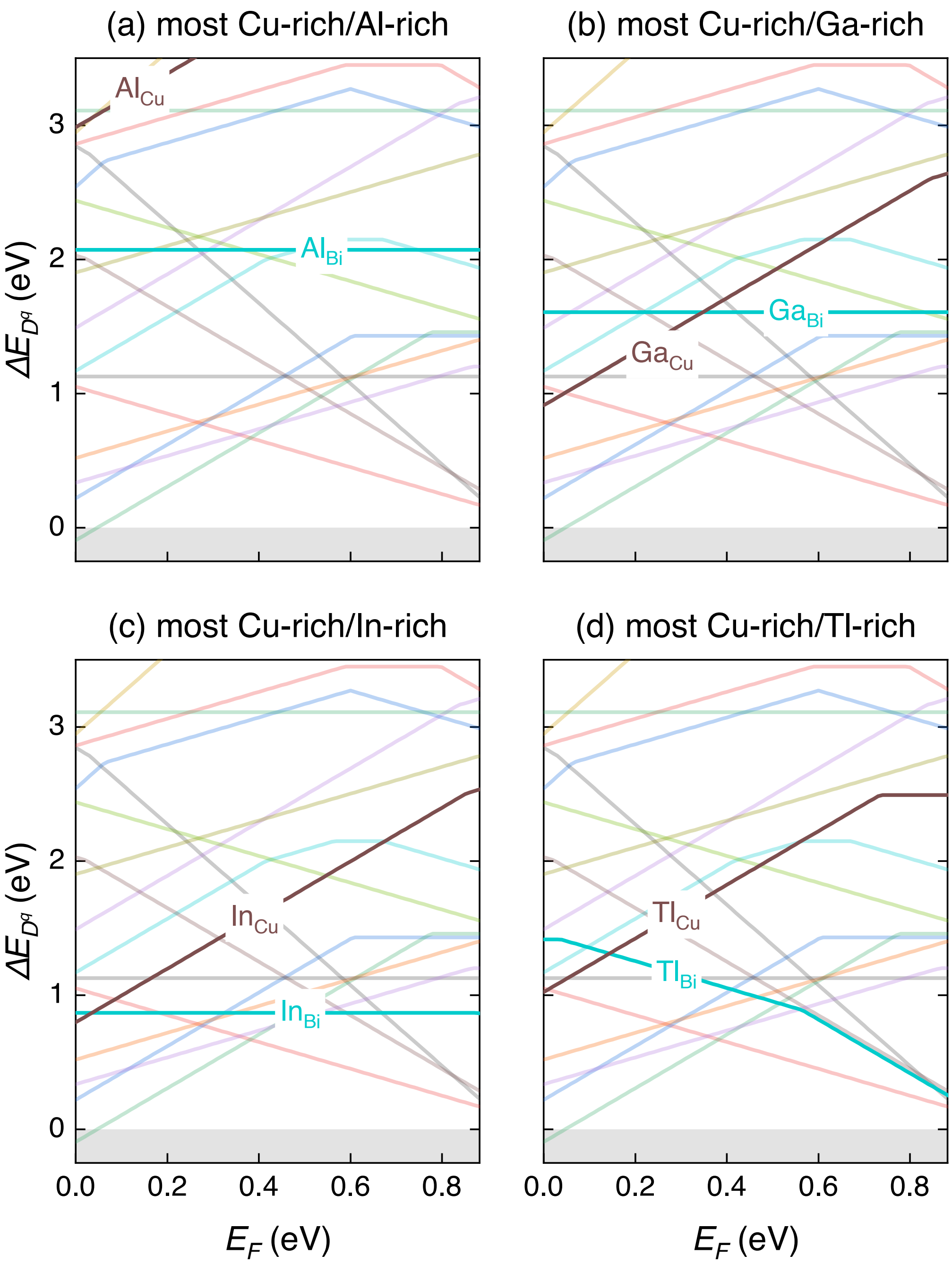

Figure S10: Formation energy of defects associated with (a) Al, (b) Ga, (c) In, and (d) Tl doping in BiCuSeO under Cu-rich conditions where BiCuSeO is in equilibrium with (a) Bi, Cu_2Se, Cu_2O, and $AlCuO_2$, (b) Bi, Cu_2Se, Cu_2O, and $CuGaO_2$, (c) Bi, Cu_2Se, Cu_2O, and $CuInO_2$, and (d) Bi, Cu_2Se, Cu_2O, and Cu_2Se_2Tl. Native defects of BiCuSeO (Figure 2 in main text) are shown in lighter colors. The equilibrium Fermi energy (E_F^{eq}), as determined by charge neutrality at 973 K, is marked with a dotted vertical line.

Group-14 Doping: Si, Ge, Sn, Pb

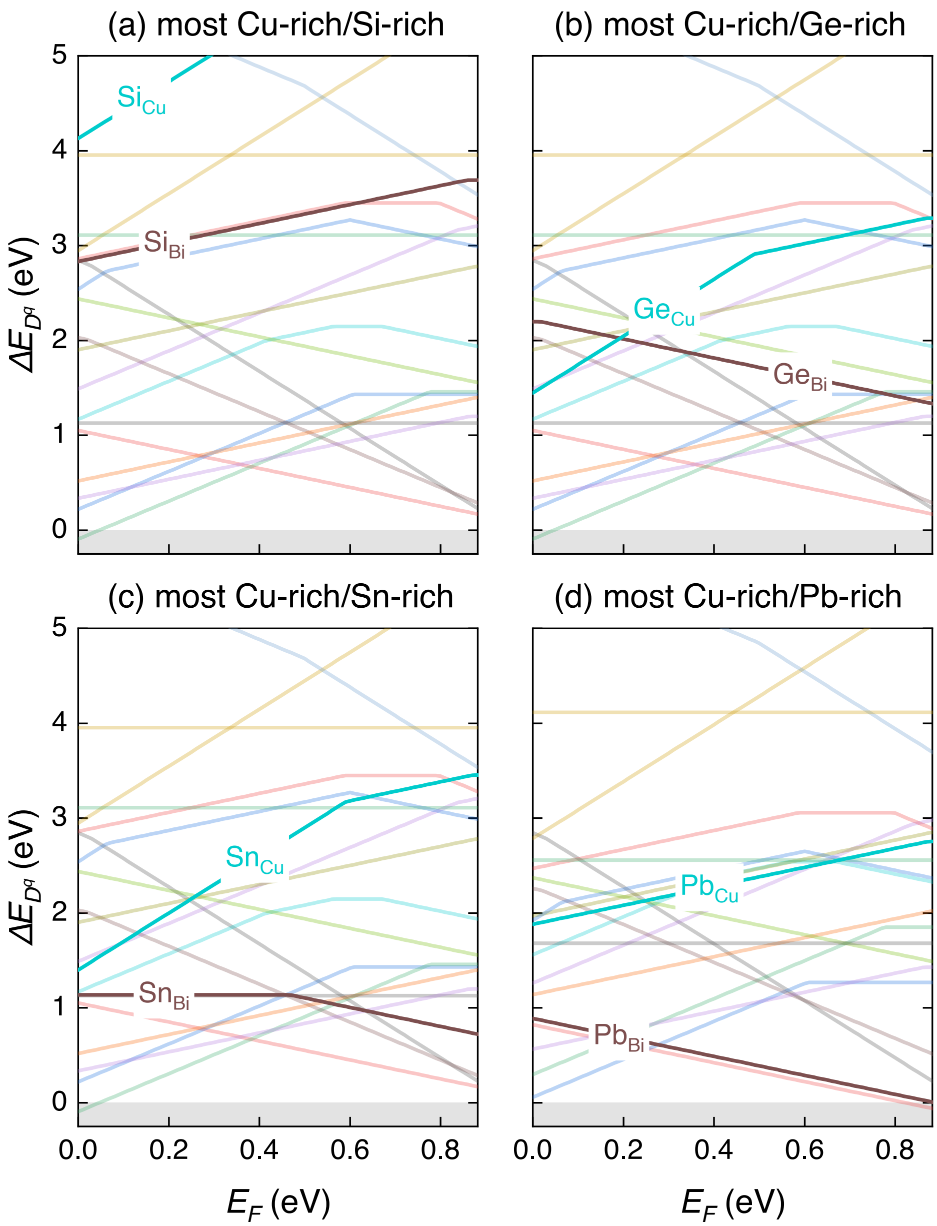

Figure S11: Formation energy of defects associated with (a) Si, (b) Ge, (c) Sn, and (d) Pb doping in BiCuSeO under Cu-rich conditions where BiCuSeO is in equilibrium with a) Bi, Cu_2Se, Cu_2O, and $Bi_4O_{12}Si_3$, (b) Bi, Cu_2Se, Cu_2O, and $Bi_4Ge_3O_{12}$, (c) Bi, Cu_2O, $Bi_2O_7Sn_2$, and Cu_2Se, and (d) Bi, PbSe, Cu_3Se_2, and Bi_2Se_3. Native defects of BiCuSeO (Figure 2 in main text) are shown in lighter colors. The equilibrium Fermi energy (E_F^{eq}), as determined by charge neutrality at 973 K, is marked with a dotted vertical line.

Phase Equilibria of Mg-Doped BiCuSeO

Equilibrium Phases	$\Delta\mu_{\mathrm{Bi}}$	$\Delta\mu_{\mathrm{Cu}}$	$\Delta\mu_{\mathrm{Mg}}$	$\Delta\mu_{\mathrm{O}}$	$\Delta\mu_{\mathrm{Se}}$	$p-n$ (cm^{-3})
Se, MgO, Cu_3Se_2, Bi_2Se_3	-0.378	-0.62	-4.323	-1.923	0.0	7.39×10^{19}
Se, MgO, Bi_2O_2Se, Bi_2O_3	-0.602	-0.708	-4.636	-1.61	0.0	1.26×10^{20}
Se, MgO, Bi_2O_2Se, Bi_2Se_3	-0.378	-0.708	-4.411	-1.835	0.0	1.25×10^{20}
Se, MgO, Cu_3Se_2, Bi_2O_3	-0.865	-0.62	-4.811	-1.435	0.0	7.53×10^{19}
Bi, MgO, Bi_2O_2Se, Bi_2Se_3	0.0	-0.582	-4.159	-2.087	-0.252	5.39×10^{19}
Bi, Cu_2Se, MgO, Cu_2O	0.0	-0.223	-4.192	-2.054	-0.643	5.24×10^{18}
Bi, MgO, Cu_2O, Bi_2O_3	0.0	-0.244	-4.234	-2.012	-0.664	5.67×10^{18}
Bi, MgO, Bi_2O_2Se, Bi_2O_3	0.0	-0.507	-4.234	-2.012	-0.402	3.45×10^{19}
Bi, MgO, Cu_3Se_2, Bi_2Se_3	0.0	-0.452	-4.03	-2.216	-0.252	2.36×10^{19}
Bi, Cu_2Se, MgO, Cu_3Se_2	0.0	-0.318	-4.097	-2.149	-0.453	1.12×10^{19}
MgO, Cu_3Se_2, Cu_2O, Bi_2O_3	-0.603	-0.445	-4.636	-1.61	-0.262	2.63×10^{19}
Cu_2Se, MgO, Cu_3Se_2, Cu_2O	-0.285	-0.318	-4.382	-1.864	-0.453	1.16×10^{19}

Table S4: Chemical potentials $\Delta\mu_{\mathrm{i}}$ (in eV) in all phase regions of the quinary Bi-Cu-Se-O-Mg phase space that are in equilibrium with BiCuSeO. The corresponding charge carrier concentration in each phase region, as determined by charge neutrality at the typical synthesis temperature of 973 K, is listed.

Phase Equilibria of Ca-Doped BiCuSeO

Equilibrium Phases	$\Delta\mu_{\mathrm{Bi}}$	$\Delta\mu_{\mathrm{Ca}}$	$\Delta\mu_{\mathrm{Cu}}$	$\Delta\mu_{\mathrm{O}}$	$\Delta\mu_{\mathrm{Se}}$	$p-n$ (cm^{-3})
Se, CaO, Cu_3Se_2, Bi_2Se_3	-0.378	-4.659	-0.62	-1.923	0.0	1.38×10^{21}
Se, CaO, CaO_3Se, Bi_2Se_3	-0.378	-4.723	-0.684	-1.859	0.0	1.19×10^{21}
Se, Bi_2O_2Se, CaO_3Se, Bi_2Se_3	-0.378	-4.795	-0.708	-1.835	0.0	8.89×10^{20}
Se, CaO, Cu_3Se_2, CaO_3Se	-0.441	-4.723	-0.62	-1.859	0.0	1.53×10^{21}
Se, Cu_3Se_2, Bi_2O_3, CaO_3Se	-0.865	-5.995	-0.62	-1.435	0.0	7.65×10^{19}
Se, Bi_2O_2Se, Bi_2O_3, CaO_3Se	-0.602	-5.47	-0.708	-1.61	0.0	1.45×10^{20}
Bi, CaO, Cu_2O, Bi_2O_3	0.0	-4.57	-0.244	-2.012	-0.664	1.11×10^{20}
Bi, CaO, Cu_2Se, Cu_2O	0.0	-4.528	-0.223	-2.054	-0.643	1.41×10^{20}
Bi, CaO, Bi_2O_2Se, Bi_2Se_3	0.0	-4.495	-0.582	-2.087	-0.252	3.88×10^{20}
Bi, CaO, Bi_2O_2Se, Bi_2O_3	0.0	-4.57	-0.507	-2.012	-0.402	2.53×10^{20}
Bi, CaO, Cu_3Se_2, Bi_2Se_3	0.0	-4.366	-0.452	-2.216	-0.252	4.48×10^{20}
Bi, CaO, Cu_2Se, Cu_3Se_2	0.0	-4.433	-0.318	-2.149	-0.453	3.44×10^{20}
CaO, Bi_2O_2Se, CaO_3Se, Bi_2Se_3	-0.354	-4.731	-0.7	-1.851	-0.016	1.05×10^{21}
CaO, Cu_2Se, Cu_2O, Cu_3Se_2	-0.285	-4.718	-0.318	-1.864	-0.453	3.95×10^{20}
CaO, Bi_2O_2Se, Bi_2O_3, CaO_3Se	-0.353	-4.806	-0.625	-1.776	-0.166	7×10^{20}
CaO, Cu_2O, Bi_2O_3, CaO_3Se	-0.485	-4.894	-0.406	-1.688	-0.341	6.1×10^{20}
Cu_2O, Cu_3Se_2, Bi_2O_3, CaO_3Se	-0.603	-5.208	-0.445	-1.61	-0.262	2.97×10^{20}
CaO, Cu_2O, Cu_3Se_2, CaO_3Se	-0.496	-4.886	-0.402	-1.696	-0.327	6.81×10^{20}

Table S5: Chemical potentials $\Delta\mu_{\mathrm{i}}$ (in eV) in all phase regions of the quinary Bi-Cu-Se-O-Ca phase space that are in equilibrium with BiCuSeO. The corresponding charge carrier concentration in each phase region, as determined by charge neutrality at the typical synthesis temperature of 973 K, is listed.

Phase Equilibria of Sr-Doped BiCuSeO

Equilibrium Phases	$\Delta\mu_{\mathrm{Bi}}$	$\Delta\mu_{\mathrm{Cu}}$	$\Delta\mu_{\mathrm{O}}$	$\Delta\mu_{\mathrm{Se}}$	$\Delta\mu_{\mathrm{Sr}}$	$p-n$ (cm^{-3})
Bi, SeSr, Cu_3Se_2, Bi_2Se_3	0.0	-0.452	-2.216	-0.252	-4.274	5.95×10^{20}
Bi, Cu_2O, Bi_2O_3, Bi_2O_4Sr	0.0	-0.244	-2.012	-0.664	-4.72	5.66×10^{19}
Bi, Cu_2Se, Cu_2O, Bi_2O_4Sr	0.0	-0.223	-2.054	-0.643	-4.551	1.2×10^{20}
Bi, Cu_2Se, $Bi_2O_5Sr_2$, Bi_2O_4Sr	0.0	-0.258	-2.089	-0.573	-4.411	2.66×10^{20}
Bi, Cu_2Se, $Bi_2O_5Sr_2$, Cu_3Se_2	0.0	-0.318	-2.149	-0.453	-4.261	6.19×10^{20}
Bi, SeSr, $Bi_2O_5Sr_2$, Cu_3Se_2	0.0	-0.386	-2.183	-0.351	-4.175	8.91×10^{20}
O_3SeSr, SeSr, Cu_3Se_2, Bi_2Se_3	-0.313	-0.591	-1.973	-0.043	-4.483	1.7×10^{21}
O_3SeSr, SeSr, $Bi_2O_5Sr_2$, Bi_2Se_3	-0.256	-0.61	-1.973	-0.081	-4.445	1.59×10^{21}
O_3SeSr, $Bi_2O_5Sr_2$, Bi_2O_4Sr, Bi_2Se_3	-0.242	-0.66	-1.927	-0.09	-4.573	1.05×10^{21}
O_3SeSr, Bi_2O_2Se, Bi_2O_4Sr, Bi_2Se_3	-0.244	-0.663	-1.924	-0.089	-4.583	1.02×10^{21}
O_3SeSr, Cu_2O, Cu_3Se_2, Bi_2O_4Sr	-0.474	-0.394	-1.712	-0.339	-4.968	4.02×10^{20}
O_3SeSr, $Bi_2O_5Sr_2$, Cu_3Se_2, Bi_2O_4Sr	-0.371	-0.445	-1.842	-0.262	-4.658	1.09×10^{21}
O_3SeSr, Cu_2O, Cu_3Se_2, Bi_2O_3	-0.603	-0.445	-1.61	-0.262	-5.353	1.29×10^{20}
O_3SeSr, SeSr, $Bi_2O_5Sr_2$, Cu_3Se_2	-0.289	-0.544	-1.973	-0.114	-4.412	1.92×10^{21}
O_3SeSr, Bi_2O_2Se, Bi_2O_3, Bi_2O_4Sr	-0.356	-0.625	-1.774	-0.164	-4.958	3.1×10^{20}
O_3SeSr, Cu_2O, Bi_2O_3, Bi_2O_4Sr	-0.487	-0.407	-1.687	-0.339	-5.045	3.03×10^{20}
Cu_2Se, $Bi_2O_5Sr_2$, Cu_3Se_2, Bi_2O_4Sr	-0.18	-0.318	-1.969	-0.453	-4.531	5.04×10^{20}
Cu_2Se, Cu_2O, Cu_3Se_2, Bi_2O_4Sr	-0.285	-0.318	-1.864	-0.453	-4.741	3.4×10^{20}
Se, O_3SeSr, Bi_2O_2Se, Bi_2O_3	-0.603	-0.708	-1.61	0.0	-5.615	1.29×10^{20}
Se, O_3SeSr, Cu_3Se_2, Bi_2O_3	-0.865	-0.62	-1.435	0.0	-6.14	7.53×10^{19}
Se, O_3SeSr, Bi_2O_2Se, Bi_2Se_3	-0.378	-0.708	-1.835	0.0	-4.94	4.03×10^{20}
Se, O_3SeSr, Cu_3Se_2, Bi_2Se_3	-0.378	-0.62	-1.923	0.0	-4.677	1.22×10^{21}

Table S6: Chemical potentials $\Delta\mu_{\mathrm{i}}$ (in eV) in all phase regions of the quinary Bi-Cu-Se-O-Sr phase space that are in equilibrium with BiCuSeO. The corresponding charge carrier concentration in each phase region, as determined by charge neutrality at the typical synthesis temperature of 973 K, is listed.

Phase Equilibria of Ba-Doped BiCuSeO

Equilibrium Phases	$\Delta\mu_{\mathrm{Ba}}$	$\Delta\mu_{\mathrm{Bi}}$	$\Delta\mu_{\mathrm{Cu}}$	$\Delta\mu_{\mathrm{O}}$	$\Delta\mu_{\mathrm{Se}}$	$p-n$ (cm^{-3})
Se, Bi_2Se_3, BaO_3Se, Cu_3Se_2	-4.722	-0.378	-0.62	-1.923	0.0	8.82×10^{19}
Se, Bi_2Se_3, Bi_2O_2Se, BaO_3Se	-4.985	-0.378	-0.708	-1.835	0.0	1.25×10^{20}
Se, BaO_3Se, Cu_3Se_2, Bi_2O_3	-6.185	-0.865	-0.62	-1.435	0.0	7.5×10^{19}
Se, Bi_2O_2Se, BaO_3Se, Bi_2O_3	-5.66	-0.603	-0.708	-1.61	0.0	1.26×10^{20}
Bi_2Se_3, BaSe, $BaBiSe_3$, $BaCu_2Se_2$	-4.399	-0.169	-0.609	-2.003	-0.139	1.12×10^{20}
Bi_2Se_3, $BaCu_2Se_2$, BaO_3Se, Cu_3Se_2	-4.643	-0.351	-0.608	-1.943	-0.018	9.45×10^{19}
Bi_2Se_3, $BaBiSe_3$, $BaCu_2Se_2$, BaO_3Se	-4.448	-0.218	-0.617	-1.979	-0.106	1.16×10^{20}
Bi_2Se_3, BaSe, Bi_2O_2Se, BaO_3Se	-4.389	-0.154	-0.633	-1.984	-0.149	1.17×10^{20}
Bi_2Se_3, BaSe, $BaBiSe_3$, BaO_3Se	-4.399	-0.169	-0.628	-1.984	-0.139	1.18×10^{20}
Cu_2O, BaO_3Se, Cu_3Se_2, $Ba_2Bi_4O_8$	-4.706	-0.372	-0.353	-1.795	-0.401	4.84×10^{19}
$BaCu_2Se_2$, BaO_3Se, Cu_3Se_2, $Ba_2Bi_4O_8$	-4.433	-0.281	-0.398	-1.908	-0.333	1.33×10^{20}
Cu_2O, BaO_3Se, Cu_3Se_2, Bi_2O_3	-5.398	-0.603	-0.445	-1.61	-0.262	2.62×10^{19}
Cu_2O, BaO_3Se, Bi_2O_3, $Ba_2Bi_4O_8$	-4.844	-0.395	-0.376	-1.748	-0.401	2.94×10^{19}
Bi_2O_2Se, BaO_3Se, Bi_2O_3, $Ba_2Bi_4O_8$	-4.757	-0.264	-0.595	-1.836	-0.226	6.61×10^{19}
BaSe, Bi_2O_2Se, BaO_3Se, $Ba_2Bi_4O_8$	-4.386	-0.153	-0.632	-1.984	-0.152	1.17×10^{20}
BaSe, $BaCu_2Se_2$, BaO_3Se, $Ba_2Bi_4O_8$	-4.357	-0.167	-0.588	-1.984	-0.181	1.28×10^{20}
BaSe, $BaBiSe_3$, $BaCu_2Se_2$, BaO_3Se	-4.412	-0.194	-0.615	-1.984	-0.126	1.2×10^{20}
$BaCu_2Se_2$, Cu_3Se_2, Cu_2Se, $Ba_2Bi_4O_8$	-4.353	-0.161	-0.318	-1.988	-0.453	8.68×10^{19}
Cu_2O, Cu_3Se_2, Cu_2Se, $Ba_2Bi_4O_8$	-4.601	-0.285	-0.318	-1.864	-0.453	4.84×10^{19}
Bi, Cu_2O, Cu_2Se, $Ba_2Bi_4O_8$	-4.411	0.0	-0.223	-2.054	-0.643	1.93×10^{19}
Bi, $BaCu_2Se_2$, Cu_2Se, $Ba_2Bi_4O_8$	-4.246	0.0	-0.264	-2.095	-0.56	5.07×10^{19}
Bi, Cu_2O, Bi_2O_3, $Ba_2Bi_4O_8$	-4.581	0.0	-0.244	-2.012	-0.664	9.38×10^{18}
Bi, $BaCu_2Se_2$, Cu_3Se_2, Cu_2Se	-4.353	0.0	-0.318	-2.149	-0.453	3.76×10^{19}
Bi, Bi_2Se_3, $BaCu_2Se_2$, Cu_3Se_2	-4.487	0.0	-0.452	-2.216	-0.252	2.87×10^{19}
Bi, BaSe, $BaCu_2Se_2$, $Ba_2Bi_4O_8$	-4.246	0.0	-0.532	-2.095	-0.292	8.36×10^{19}
Bi, Bi_2O_2Se, Bi_2O_3, $Ba_2Bi_4O_8$	-4.581	0.0	-0.507	-2.012	-0.402	3.6×10^{19}
Bi, BaSe, Bi_2O_2Se, $Ba_2Bi_4O_8$	-4.284	0.0	-0.581	-2.086	-0.254	8.02×10^{19}
Bi, Bi_2Se_3, BaSe, Bi_2O_2Se	-4.286	0.0	-0.582	-2.087	-0.252	8×10^{19}
Bi, Bi_2Se_3, BaSe, $BaCu_2Se_2$	-4.286	0.0	-0.553	-2.116	-0.252	7.29×10^{19}

Table S7: Chemical potentials $\Delta\mu_{\rm i}$ (in eV) in all phase regions of the quinary Bi-Cu-Se-O-Ba phase space that are in equilibrium with BiCuSeO. The corresponding charge carrier concentration in each phase region, as determined by charge neutrality at the typical synthesis temperature of 973 K, is listed.

Phase Equilibriua of Li-Doped BiCuSeO

Equilibrium Phases	$\Delta\mu_{\mathrm{Bi}}$	$\Delta\mu_{\mathrm{Cu}}$	$\Delta\mu_{\mathrm{Li}}$	$\Delta\mu_{\mathrm{O}}$	$\Delta\mu_{\mathrm{Se}}$	$p-n$ (cm^{-3})
Se, Cu_3Se_2, Bi_2Se_3, $Bi_8Li_{24}O_{24}$	-0.378	-0.62	-2.217	-1.923	0.0	1.12×10^{20}
Se, Bi_2O_2Se, Bi_2O_3, $BiLiO_2$	-0.603	-0.708	-2.509	-1.61	0.0	1.44×10^{20}
Se, Bi_2O_2Se, $BiLiO_2$, $Bi_8Li_{24}O_{24}$	-0.438	-0.708	-2.345	-1.775	0.0	1.22×10^{20}
Se, Bi_2O_2Se, Bi_2Se_3, $Bi_8Li_{24}O_{24}$	-0.378	-0.708	-2.305	-1.835	0.0	1.09×10^{20}
Se, Li_4O_5Se, Cu_3Se_2, $Bi_8Li_{24}O_{24}$	-0.609	-0.62	-2.372	-1.691	0.0	1.75×10^{20}
Se, Li_4O_5Se, Cu_3Se_2, Bi_2O_3	-0.865	-0.62	-2.691	-1.435	0.0	1.48×10^{20}
Se, Li_4O_5Se, $BiLiO_2$, $Bi_8Li_{24}O_{24}$	-0.594	-0.655	-2.397	-1.671	0.0	1.57×10^{20}
Se, Li_4O_5Se, Bi_2O_3, $BiLiO_2$	-0.676	-0.683	-2.534	-1.561	0.0	1.48×10^{20}
Bi, Bi_2O_2Se, Bi_2Se_3, $Bi_8Li_{24}O_{24}$	0.0	-0.582	-2.179	-2.087	-0.252	4.61×10^{19}
Bi, $BiLiO_2$, $Cu_8Li_8O_8$, $Bi_8Li_{24}O_{24}$	0.0	-0.329	-2.199	-2.067	-0.525	2.62×10^{19}
Bi, Bi_2O_2Se, $BiLiO_2$, $Bi_8Li_{24}O_{24}$	0.0	-0.562	-2.199	-2.067	-0.292	4.48×10^{19}
Bi, Bi_2O_2Se, Bi_2O_3, $BiLiO_2$	0.0	-0.507	-2.309	-2.012	-0.402	3.57×10^{19}
Bi, Bi_2O_3, $BiLiO_2$, $Cu_8Li_8O_8$	0.0	-0.274	-2.309	-2.012	-0.634	1.53×10^{19}
Bi, Cu_2O, Bi_2O_3, $Cu_8Li_8O_8$	0.0	-0.244	-2.338	-2.012	-0.664	1.28×10^{19}
Bi, Cu_2Se, Cu_2O, $Cu_8Li_8O_8$	0.0	-0.223	-2.317	-2.054	-0.643	1.41×10^{19}
Bi, Cu_3Se_2, Bi_2Se_3, $Bi_8Li_{24}O_{24}$	0.0	-0.452	-2.049	-2.216	-0.252	4.26×10^{19}
Bi, Cu_2Se, Cu_3Se_2, $Cu_8Li_8O_8$	0.0	-0.318	-2.127	-2.149	-0.453	3.45×10^{19}
Bi, Cu_3Se_2, $Cu_8Li_8O_8$, $Bi_8Li_{24}O_{24}$	0.0	-0.329	-2.111	-2.155	-0.437	3.66×10^{19}
Cu_3Se_2, $BiLiO_2$, $Cu_8Li_8O_8$, $Bi_8Li_{24}O_{24}$	-0.527	-0.505	-2.375	-1.715	-0.173	1.23×10^{20}
Cu_3Se_2, Bi_2O_3, $BiLiO_2$, $Cu_8Li_8O_8$	-0.692	-0.505	-2.539	-1.55	-0.173	1.25×10^{20}
Cu_2O, Cu_3Se_2, Bi_2O_3, $Cu_8Li_8O_8$	-0.603	-0.445	-2.539	-1.61	-0.262	8.63×10^{19}
Li_4O_5Se, Cu_3Se_2, Bi_2O_3, $BiLiO_2$	-0.739	-0.536	-2.555	-1.519	-0.126	1.43×10^{20}
Li_4O_5Se, Cu_3Se_2, $BiLiO_2$, $Bi_8Li_{24}O_{24}$	-0.63	-0.573	-2.409	-1.647	-0.071	1.65×10^{20}
Cu_2Se, Cu_2O, Cu_3Se_2, $Cu_8Li_8O_8$	-0.285	-0.318	-2.412	-1.864	-0.453	3.66×10^{19}

Table S8: Chemical potentials $\Delta\mu_{\mathrm{i}}$ (in eV) in all phase regions of the quinary Bi-Cu-Se-O-Li phase space that are in equilibrium with BiCuSeO. The corresponding charge carrier concentration in each phase region, as determined by charge neutrality at the typical synthesis temperature of 973 K, is listed.

Phase Equilibriua of Zn-Doped BiCuSeO

Equilibrium Phases	$\Delta\mu_{\text{Bi}}$	$\Delta\mu_{\text{Cu}}$	$\Delta\mu_{\text{O}}$	$\Delta\mu_{\text{Se}}$	$\Delta\mu_{\text{Zn}}$	$p - n$ (cm^{-3})
Bi, Bi_2O_2Se, Bi_2Se_3, SeZn	0.0	-0.582	-2.087	-0.252	-1.496	6.54×10^{18}
Bi, Bi_2O_2Se, SeZn, OZn	0.0	-0.579	-2.084	-0.256	-1.492	6.37×10^{18}
Bi, Cu_2Se, Cu_2O, OZn	0.0	-0.223	-2.054	-0.643	-1.522	4.3×10^{18}
Bi, Cu_2O, Bi_2O_3, OZn	0.0	-0.244	-2.012	-0.664	-1.564	4.94×10^{18}
Bi, Bi_2O_2Se, Bi_2O_3, OZn	0.0	-0.507	-2.012	-0.402	-1.564	9.63×10^{18}
Bi, Bi_2Se_3, Cu_3Se_2, SeZn	0.0	-0.452	-2.216	-0.252	-1.496	6.37×10^{18}
Bi, Cu_3Se_2, SeZn, OZn	0.0	-0.384	-2.182	-0.354	-1.394	3.33×10^{18}
Bi, Cu_2Se, Cu_3Se_2, OZn	0.0	-0.318	-2.149	-0.453	-1.427	3.99×10^{18}
Cu_2Se, Cu_2O, Cu_3Se_2, OZn	-0.285	-0.318	-1.864	-0.453	-1.712	1.04×10^{19}
Cu_2O, Cu_3Se_2, Bi_2O_3, OZn	-0.603	-0.445	-1.61	-0.262	-1.966	2.55×10^{19}
Se, Cu_3Se_2, Bi_2O_3, OZn	-0.865	-0.62	-1.435	0.0	-2.141	7.29×10^{19}
Se, Bi_2O_2Se, Bi_2Se_3, SeZn	-0.378	-0.708	-1.835	0.0	-1.748	2.89×10^{19}
Se, Bi_2O_2Se, SeZn, OZn	-0.385	-0.708	-1.828	0.0	-1.748	2.89×10^{19}
Se, Bi_2O_2Se, Bi_2O_3, OZn	-0.603	-0.708	-1.61	0.0	-1.966	8.07×10^{19}
Se, Bi_2Se_3, Cu_3Se_2, SeZn	-0.378	-0.62	-1.923	0.0	-1.748	2.76×10^{19}
Se, Cu_3Se_2, SeZn, OZn	-0.472	-0.62	-1.828	0.0	-1.748	2.77×10^{19}

Table S9: Chemical potentials $\Delta\mu_{\text{i}}$ (in eV) in all phase regions of the quinary Bi-Cu-Se-O-Zn phase space that are in equilibrium with BiCuSeO. The corresponding charge carrier concentration in each phase region, as determined by charge neutrality at the typical synthesis temperature of 973 K, is listed.

Phase Equilibriua of Al-Doped BiCuSeO

Equilibrium Phases	$\Delta\mu_{Al}$	$\Delta\mu_{Bi}$	$\Delta\mu_{Cu}$	$\Delta\mu_{O}$	$\Delta\mu_{Se}$	$p-n$ (cm^{-3})
Se, Al_2O_3, Bi_2Se_3, Cu_3Se_2	-5.916	-0.378	-0.62	-1.923	0.0	7.36×10^{19}
Se, Bi_2O_2Se, Bi_2O_3, $Al_4Bi_2O_9$	-6.484	-0.602	-0.708	-1.61	0.0	1.26×10^{20}
Se, Bi_2O_2Se, Bi_2Se_3, $Al_4Bi_2O_9$	-6.09	-0.378	-0.708	-1.835	0.0	1.25×10^{20}
Se, Al_2O_3, Bi_2Se_3, $Al_4Bi_2O_9$	-5.962	-0.378	-0.651	-1.892	0.0	8.88×10^{19}
Se, Al_2O_3, Cu_3Se_2, $Al_4Bi_2O_9$	-6.055	-0.47	-0.62	-1.83	0.0	7.46×10^{19}
Se, Cu_3Se_2, Bi_2O_3, $Al_4Bi_2O_9$	-6.746	-0.865	-0.62	-1.435	0.0	7.5×10^{19}
Cu_2O, Cu_3Se_2, $AlCuO_2$, Bi_2O_3	-6.523	-0.603	-0.445	-1.61	-0.262	2.61×10^{19}
Cu_3Se_2, $AlCuO_2$, Bi_2O_3, $Al_4Bi_2O_9$	-6.602	-0.721	-0.524	-1.531	-0.145	4.22×10^{19}
Al_2O_3, Cu_3Se_2, $AlCuO_2$, $Al_4Bi_2O_9$	-5.614	-0.029	-0.326	-2.124	-0.441	1.17×10^{19}
Cu_2Se, Cu_2O, Cu_3Se_2, $AlCuO_2$	-6.142	-0.285	-0.318	-1.864	-0.453	1.13×10^{19}
Cu_2Se, Al_2O_3, Cu_3Se_2, $AlCuO_2$	-5.59	-0.009	-0.318	-2.14	-0.453	1.1×10^{19}
Bi, Cu_2Se, Al_2O_3, Cu_3Se_2	-5.576	0.0	-0.318	-2.149	-0.453	1.1×10^{19}
Bi, Al_2O_3, Bi_2Se_3, Cu_3Se_2	-5.476	0.0	-0.452	-2.216	-0.252	2.34×10^{19}
Bi, Cu_2Se, Cu_2O, $AlCuO_2$	-5.857	0.0	-0.223	-2.054	-0.643	5.11×10^{18}
Bi, Cu_2Se, Al_2O_3, $AlCuO_2$	-5.581	0.0	-0.315	-2.146	-0.459	1.08×10^{19}
Bi, Al_2O_3, $AlCuO_2$, $Al_4Bi_2O_9$	-5.585	0.0	-0.316	-2.143	-0.46	1.08×10^{19}
Bi, $AlCuO_2$, Bi_2O_3, $Al_4Bi_2O_9$	-5.881	0.0	-0.283	-2.012	-0.625	7.59×10^{18}
Bi, Cu_2O, $AlCuO_2$, Bi_2O_3	-5.92	0.0	-0.244	-2.012	-0.664	5.61×10^{18}
Bi, Bi_2O_2Se, Bi_2O_3, $Al_4Bi_2O_9$	-5.881	0.0	-0.507	-2.012	-0.402	3.45×10^{19}
Bi, Bi_2O_2Se, Bi_2Se_3, $Al_4Bi_2O_9$	-5.712	0.0	-0.582	-2.087	-0.252	5.39×10^{19}
Bi, Al_2O_3, Bi_2Se_3, $Al_4Bi_2O_9$	-5.585	0.0	-0.525	-2.143	-0.252	3.77×10^{19}

Table S10: Chemical potentials $\Delta\mu_i$ (in eV) in all phase regions of the quinary Bi-Cu-Se-O-Al phase space that are in equilibrium with BiCuSeO. The corresponding charge carrier concentration in each phase region, as determined by charge neutrality at the typical synthesis temperature of 973 K, is listed.

Phase Equilibriua of Ga-Doped BiCuSeO

Equilibrium Phases	$\Delta\mu_{\mathrm{Bi}}$	$\Delta\mu_{\mathrm{Cu}}$	$\Delta\mu_{\mathrm{Ga}}$	$\Delta\mu_{\mathrm{O}}$	$\Delta\mu_{\mathrm{Se}}$	$p-n$ (cm^{-3})
Se, Cu_3Se_2, Ga_2O_3, Bi_2Se_3	-0.378	-0.62	-2.811	-1.923	0.0	7.36×10^{19}
Se, Bi_2O_2Se, $Bi_2Ga_4O_9$, Bi_2O_3	-0.602	-0.708	-3.341	-1.61	0.0	1.26×10^{20}
Se, $Bi_2Ga_4O_9$, Ga_2O_3, Bi_2Se_3	-0.378	-0.701	-2.933	-1.842	0.0	1.19×10^{20}
Se, Bi_2O_2Se, $Bi_2Ga_4O_9$, Bi_2Se_3	-0.378	-0.708	-2.948	-1.835	0.0	1.24×10^{20}
Se, $Bi_2Ga_4O_9$, Cu_3Se_2, Ga_2O_3	-0.62	-0.62	-3.175	-1.68	0.0	7.48×10^{19}
Se, $Bi_2Ga_4O_9$, Cu_3Se_2, Bi_2O_3	-0.865	-0.62	-3.604	-1.435	0.0	7.5×10^{19}
Bi, Cu_2O, $CuGaO_2$, Bi_2O_3	0.0	-0.244	-2.754	-2.012	-0.664	5.61×10^{18}
Bi, Bi_2O_2Se, $Bi_2Ga_4O_9$, Bi_2Se_3	0.0	-0.582	-2.57	-2.087	-0.252	5.37×10^{19}
Bi, $Bi_2Ga_4O_9$, Ga_2O_3, Bi_2Se_3	0.0	-0.575	-2.555	-2.093	-0.252	5.14×10^{19}
Bi, Bi_2O_2Se, $Bi_2Ga_4O_9$, Bi_2O_3	0.0	-0.507	-2.739	-2.012	-0.402	3.45×10^{19}
Bi, $CuGaO_2$, $Bi_2Ga_4O_9$, Ga_2O_3	0.0	-0.28	-2.555	-2.093	-0.546	8.27×10^{18}
Bi, $CuGaO_2$, $Bi_2Ga_4O_9$, Bi_2O_3	0.0	-0.26	-2.739	-2.012	-0.648	6.37×10^{18}
Bi, Cu_2Se, $CuGaO_2$, Ga_2O_3	0.0	-0.274	-2.537	-2.105	-0.54	8×10^{18}
Bi, Cu_2Se, Cu_2O, $CuGaO_2$	0.0	-0.223	-2.691	-2.054	-0.643	5.11×10^{18}
Bi, Cu_3Se_2, Ga_2O_3, Bi_2Se_3	0.0	-0.452	-2.371	-2.216	-0.252	2.33×10^{19}
Bi, Cu_2Se, Cu_3Se_2, Ga_2O_3	0.0	-0.318	-2.471	-2.149	-0.453	1.1×10^{19}
$CuGaO_2$, $Bi_2Ga_4O_9$, Cu_3Se_2, Ga_2O_3	-0.221	-0.354	-2.776	-1.946	-0.399	1.44×10^{19}
$CuGaO_2$, $Bi_2Ga_4O_9$, Cu_3Se_2, Bi_2O_3	-0.65	-0.477	-3.389	-1.578	-0.215	3.17×10^{19}
Cu_2O, $CuGaO_2$, Cu_3Se_2, Bi_2O_3	-0.603	-0.445	-3.357	-1.61	-0.262	2.61×10^{19}
Cu_2Se, Cu_2O, $CuGaO_2$, Cu_3Se_2	-0.285	-0.318	-2.976	-1.864	-0.453	1.13×10^{19}
Cu_2Se, $CuGaO_2$, Cu_3Se_2, Ga_2O_3	-0.131	-0.318	-2.668	-2.018	-0.453	1.13×10^{19}

Table S11: Chemical potentials $\Delta\mu_{\mathrm{i}}$ (in eV) in all phase regions of the quinary Bi-Cu-Se-O-Ga phase space that are in equilibrium with BiCuSeO. The corresponding charge carrier concentration in each phase region, as determined by charge neutrality at the typical synthesis temperature of 973 K, is listed.

Phase Equilibriua of In-Doped BiCuSeO

Equilibrium Phases	$\Delta\mu_{\mathrm{Bi}}$	$\Delta\mu_{\mathrm{Cu}}$	$\Delta\mu_{\mathrm{In}}$	$\Delta\mu_{\mathrm{O}}$	$\Delta\mu_{\mathrm{Se}}$	$p-n$ (cm^{-3})
Se, In_2O_3, Cu_3Se_2, $CuInSe_2$	-0.379	-0.62	-1.896	-1.921	0.0	7.34×10^{19}
Se, Cu_3Se_2, $CuInSe_2$, Bi_2Se_3	-0.378	-0.62	-1.896	-1.923	0.0	7.34×10^{19}
Se, In_2O_3, Bi_2O_2Se, Bi_2O_3	-0.602	-0.708	-2.362	-1.61	0.0	1.26×10^{20}
Se, In_2O_3, $CuInSe_2$, Bi_2Se_3	-0.378	-0.621	-1.895	-1.922	0.0	7.39×10^{19}
Se, In_2O_3, Bi_2O_2Se, Bi_2Se_3	-0.378	-0.708	-2.025	-1.835	0.0	1.24×10^{20}
Se, In_2O_3, Cu_3Se_2, Bi_2O_3	-0.865	-0.62	-2.625	-1.435	0.0	7.48×10^{19}
Bi, In_2O_3, Bi_2O_2Se, Bi_2Se_3	0.0	-0.582	-1.648	-2.087	-0.252	5.36×10^{19}
Bi, In_2O_3, $CuInSe_2$, Bi_2Se_3	0.0	-0.495	-1.518	-2.173	-0.252	3.08×10^{19}
Bi, In_2O_3, Bi_2O_2Se, Bi_2O_3	0.0	-0.507	-1.76	-2.012	-0.402	3.45×10^{19}
Bi, Cu_2Se, In_2O_3, $CuInO_2$	0.0	-0.223	-1.696	-2.054	-0.642	5.13×10^{18}
Bi, Cu_2Se, Cu_2O, $CuInO_2$	0.0	-0.223	-1.697	-2.054	-0.643	5.11×10^{18}
Bi, Cu_2O, $CuInO_2$, Bi_2O_3	0.0	-0.244	-1.76	-2.012	-0.664	5.61×10^{18}
Bi, In_2O_3, $CuInO_2$, Bi_2O_3	0.0	-0.245	-1.76	-2.012	-0.664	5.65×10^{18}
Bi, Cu_3Se_2, $CuInSe_2$, Bi_2Se_3	0.0	-0.452	-1.56	-2.216	-0.252	2.33×10^{19}
Bi, In_2O_3, Cu_3Se_2, $CuInSe_2$	0.0	-0.413	-1.482	-2.197	-0.31	1.91×10^{19}
Bi, Cu_2Se, In_2O_3, Cu_3Se_2	0.0	-0.318	-1.554	-2.149	-0.453	1.1×10^{19}
In_2O_3, $CuInO_2$, Cu_3Se_2, Bi_2O_3	-0.604	-0.446	-2.364	-1.609	-0.261	2.62×10^{19}
Cu_2O, $CuInO_2$, Cu_3Se_2, Bi_2O_3	-0.603	-0.445	-2.363	-1.61	-0.262	2.6×10^{19}
Cu_2Se, In_2O_3, $CuInO_2$, Cu_3Se_2	-0.284	-0.318	-1.98	-1.865	-0.453	1.13×10^{19}
Cu_2Se, Cu_2O, $CuInO_2$, Cu_3Se_2	-0.285	-0.318	-1.982	-1.864	-0.453	1.13×10^{19}

Table S12: Chemical potentials $\Delta\mu_{\mathrm{i}}$ (in eV) in all phase regions of the quinary Bi-Cu-Se-O-In phase space that are in equilibrium with BiCuSeO. The corresponding charge carrier concentration in each phase region, as determined by charge neutrality at the typical synthesis temperature of 973 K, is listed.

Phase Equilibriua of Tl-Doped BiCuSeO

Equilibrium Phases	$\Delta\mu_{\mathrm{Bi}}$	$\Delta\mu_{\mathrm{Cu}}$	$\Delta\mu_{\mathrm{O}}$	$\Delta\mu_{\mathrm{Se}}$	$\Delta\mu_{\mathrm{Tl}}$	$p-n$ (cm^{-3})
Bi, Bi_2O_2Se, $BiSe_2Tl$, Bi_2Se_3	0.0	-0.582	-2.087	-0.252	-0.659	5.39×10^{19}
Bi, $BiSe_2Tl$, Bi_2O_3, $Se_{12}Tl_{20}$	0.0	-0.41	-2.012	-0.498	-0.166	1.85×10^{19}
Bi, Bi_2O_2Se, $BiSe_2Tl$, Bi_2O_3	0.0	-0.507	-2.012	-0.402	-0.359	3.45×10^{19}
Bi, $BiSe_2Tl$, Cu_3Se_2, Bi_2Se_3	0.0	-0.452	-2.216	-0.252	-0.659	2.34×10^{19}
Bi, $BiSe_2Tl$, $Se_{12}Tl_{20}$, Cu_2Se_2Tl	0.0	-0.399	-2.023	-0.498	-0.166	1.74×10^{19}
Bi, Bi_2O_3, $Se_{12}Tl_{20}$, Cu_2Se_2Tl	0.0	-0.372	-2.012	-0.537	-0.142	1.43×10^{19}
Bi, Cu_2O, Bi_2O_3, Cu_2Se_2Tl	0.0	-0.244	-2.012	-0.664	-0.142	5.67×10^{18}
Bi, Cu_2Se, Cu_2O, Cu_2Se_2Tl	0.0	-0.223	-2.054	-0.643	-0.227	5.15×10^{18}
Bi, $BiSe_2Tl$, Cu_3Se_2, Cu_2Se_2Tl	0.0	-0.399	-2.189	-0.332	-0.498	1.78×10^{19}
Bi, Cu_2Se, Cu_3Se_2, Cu_2Se_2Tl	0.0	-0.318	-2.149	-0.453	-0.417	1.1×10^{19}
$BiSe_2Tl$, Bi_2O_3, $Se_{12}Tl_{20}$, Cu_2Se_2Tl	-0.097	-0.447	-1.947	-0.429	-0.207	2.44×10^{19}
Cu_2Se, Cu_2O, Cu_3Se_2, Cu_2Se_2Tl	-0.285	-0.318	-1.864	-0.453	-0.417	1.14×10^{19}
Cu_2O, Cu_3Se_2, Bi_2O_3, Cu_2Se_2Tl	-0.603	-0.445	-1.61	-0.262	-0.544	2.62×10^{19}
Se, Cu_3Se_2, Bi_2O_3, Cu_2Se_2Tl	-0.865	-0.62	-1.435	0.0	-0.719	7.53×10^{19}
Se, $BiSe_2Tl$, Bi_2O_3, Cu_2Se_2Tl	-0.612	-0.704	-1.604	0.0	-0.55	1.23×10^{20}
Se, Bi_2O_2Se, $BiSe_2Tl$, Bi_2Se_3	-0.378	-0.708	-1.835	0.0	-0.784	1.25×10^{20}
Se, Bi_2O_2Se, $BiSe_2Tl$, Bi_2O_3	-0.602	-0.708	-1.61	0.0	-0.56	1.26×10^{20}
Se, $BiSe_2Tl$, Cu_3Se_2, Bi_2Se_3	-0.378	-0.62	-1.923	0.0	-0.784	7.36×10^{19}
Se, $BiSe_2Tl$, Cu_3Se_2, Cu_2Se_2Tl	-0.443	-0.62	-1.857	0.0	-0.719	7.43×10^{19}

Table S13: Chemical potentials $\Delta\mu_{\mathrm{i}}$ (in eV) in all phase regions of the quinary Bi-Cu-Se-O-Tl phase space that are in equilibrium with BiCuSeO. The corresponding charge carrier concentration in each phase region, as determined by charge neutrality at the typical synthesis temperature of 973 K, is listed.

Phase Equilibriua of Si-Doped BiCuSeO

Equilibrium Phases	$\Delta\mu_{Bi}$	$\Delta\mu_{Cu}$	$\Delta\mu_{O}$	$\Delta\mu_{Se}$	$\Delta\mu_{Si}$	$p-n$ (cm^{-3})
Bi, $Bi_4O_{12}Si_3$, Bi_2Se_3, O_2Si	0.0	-0.491	-2.177	-0.252	-5.116	3.02×10^{19}
Bi, $Bi_4O_{12}Si_3$, Bi_2O_2Se, Bi_2Se_3	0.0	-0.582	-2.087	-0.252	-5.477	5.39×10^{19}
Bi, Cu_2O, $Bi_4O_{12}Si_3$, Bi_2O_3	0.0	-0.244	-2.012	-0.664	-5.777	5.61×10^{18}
Bi, $Bi_4O_{12}Si_3$, Bi_2O_2Se, Bi_2O_3	0.0	-0.507	-2.012	-0.402	-5.777	3.45×10^{19}
Bi, Cu_2Se, Cu_2O, $Bi_4O_{12}Si_3$	0.0	-0.223	-2.054	-0.643	-5.608	5.11×10^{18}
Bi, Cu_3Se_2, Bi_2Se_3, O_2Si	0.0	-0.452	-2.216	-0.252	-5.038	2.34×10^{19}
Bi, $Bi_4O_{12}Si_3$, Cu_3Se_2, O_2Si	0.0	-0.374	-2.177	-0.369	-5.116	1.55×10^{19}
Bi, Cu_2Se, $Bi_4O_{12}Si_3$, Cu_3Se_2	0.0	-0.318	-2.149	-0.453	-5.228	1.1×10^{19}
$Bi_4O_{12}Si_3$, Cu_3Se_2, Bi_2Se_3, O_2Si	-0.352	-0.609	-1.942	-0.017	-5.586	6.87×10^{19}
Cu_2Se, Cu_2O, $Bi_4O_{12}Si_3$, Cu_3Se_2	-0.285	-0.318	-1.864	-0.453	-5.988	1.13×10^{19}
Cu_2O, $Bi_4O_{12}Si_3$, Cu_3Se_2, Bi_2O_3	-0.603	-0.445	-1.61	-0.262	-6.581	2.61×10^{19}
Se, $Bi_4O_{12}Si_3$, Cu_3Se_2, Bi_2O_3	-0.865	-0.62	-1.435	0.0	-6.931	7.5×10^{19}
Se, $Bi_4O_{12}Si_3$, Cu_3Se_2, Bi_2Se_3	-0.378	-0.62	-1.923	0.0	-5.63	7.36×10^{19}
Se, $Bi_4O_{12}Si_3$, Bi_2O_2Se, Bi_2Se_3	-0.378	-0.708	-1.835	0.0	-5.981	1.25×10^{20}
Se, $Bi_4O_{12}Si_3$, Bi_2O_2Se, Bi_2O_3	-0.603	-0.708	-1.61	0.0	-6.581	1.26×10^{20}

Table S14: Chemical potentials $\Delta\mu_i$ (in eV) in all phase regions of the quinary Bi-Cu-Se-O-Si phase space that are in equilibrium with BiCuSeO. The corresponding charge carrier concentration in each phase region, as determined by charge neutrality at the typical synthesis temperature of 973 K, is listed.

Phase Equilibriua of Ge-Doped BiCuSeO

Equilibrium Phases	$\Delta\mu_{\mathrm{Bi}}$	$\Delta\mu_{\mathrm{Cu}}$	$\Delta\mu_{\mathrm{Ge}}$	$\Delta\mu_{\mathrm{O}}$	$\Delta\mu_{\mathrm{Se}}$	$p-n$ (cm^{-3})
Se, $Bi_4Ge_3O_{12}$, Cu_3Se_2, Bi_2Se_3	-0.378	-0.62	-2.165	-1.923	0.0	7.36×10^{19}
Se, $Bi_{12}GeO_{20}$, Bi_2O_2Se, $Bi_4Ge_3O_{12}$	-0.582	-0.708	-3.061	-1.63	0.0	1.26×10^{20}
Se, $Bi_{12}GeO_{20}$, Bi_2O_2Se, Bi_2O_3	-0.603	-0.708	-3.224	-1.61	0.0	1.26×10^{20}
Se, Bi_2O_2Se, $Bi_4Ge_3O_{12}$, Bi_2Se_3	-0.378	-0.708	-2.515	-1.835	0.0	1.25×10^{20}
Se, $Bi_{12}GeO_{20}$, Cu_3Se_2, Bi_2O_3	-0.865	-0.62	-3.574	-1.435	0.0	7.5×10^{19}
Se, $Bi_{12}GeO_{20}$, $Bi_4Ge_3O_{12}$, Cu_3Se_2	-0.845	-0.62	-3.411	-1.455	0.0	7.48×10^{19}
Bi, Bi_2O_2Se, $Bi_4Ge_3O_{12}$, Bi_2Se_3	0.0	-0.582	-2.012	-2.087	-0.252	5.39×10^{19}
Bi, $Bi_{12}GeO_{20}$, Bi_2O_2Se, Bi_2O_3	0.0	-0.507	-2.421	-2.012	-0.402	3.45×10^{19}
Bi, $Bi_{12}GeO_{20}$, Bi_2O_2Se, $Bi_4Ge_3O_{12}$	0.0	-0.514	-2.284	-2.018	-0.388	3.62×10^{19}
Bi, $Bi_4Ge_3O_{12}$, Cu_3Se_2, Bi_2Se_3	0.0	-0.452	-1.494	-2.216	-0.252	2.34×10^{19}
Bi, Cu_2Se, $Bi_4Ge_3O_{12}$, Cu_3Se_2	0.0	-0.318	-1.762	-2.149	-0.453	1.1×10^{19}
Bi, Cu_2Se, Cu_2O, $Bi_4Ge_3O_{12}$	0.0	-0.223	-2.142	-2.054	-0.643	5.11×10^{18}
Bi, $Bi_{12}GeO_{20}$, Cu_2O, Bi_2O_3	0.0	-0.244	-2.421	-2.012	-0.664	5.61×10^{18}
Bi, $Bi_{12}GeO_{20}$, Cu_2O, $Bi_4Ge_3O_{12}$	0.0	-0.241	-2.284	-2.018	-0.661	5.54×10^{18}
Cu_2Se, Cu_2O, $Bi_4Ge_3O_{12}$, Cu_3Se_2	-0.285	-0.318	-2.522	-1.864	-0.453	1.13×10^{19}
$Bi_{12}GeO_{20}$, Cu_2O, Cu_3Se_2, Bi_2O_3	-0.603	-0.445	-3.224	-1.61	-0.262	2.61×10^{19}
$Bi_{12}GeO_{20}$, Cu_2O, $Bi_4Ge_3O_{12}$, Cu_3Se_2	-0.552	-0.425	-3.02	-1.651	-0.293	2.3×10^{19}

Table S15: Chemical potentials $\Delta\mu_{\mathrm{i}}$ (in eV) in all phase regions of the quinary Bi-Cu-Se-O-Ge phase space that are in equilibrium with BiCuSeO. The corresponding charge carrier concentration in each phase region, as determined by charge neutrality at the typical synthesis temperature of 973 K, is listed.

Phase Equilibriua of Sn-Doped BiCuSeO

Equilibrium Phases	$\Delta\mu_{\mathrm{Bi}}$	$\Delta\mu_{\mathrm{Cu}}$	$\Delta\mu_{\mathrm{O}}$	$\Delta\mu_{\mathrm{Se}}$	$\Delta\mu_{\mathrm{Sn}}$	$p-n$ (cm^{-3})
Se, O_2Sn, Cu_3Se_2, Bi_2Se_3	-0.378	-0.62	-1.923	0.0	-1.897	7.36×10^{19}
Se, Bi_2O_2Se, $Bi_2O_7Sn_2$, Bi_2O_3	-0.603	-0.708	-1.61	0.0	-2.676	1.26×10^{20}
Se, Bi_2O_2Se, $Bi_2O_7Sn_2$, Bi_2Se_3	-0.378	-0.708	-1.835	0.0	-2.113	1.25×10^{20}
Se, O_2Sn, $Bi_2O_7Sn_2$, Bi_2Se_3	-0.378	-0.68	-1.863	0.0	-2.017	1.06×10^{20}
Se, O_2Sn, $Bi_2O_7Sn_2$, Cu_3Se_2	-0.557	-0.62	-1.743	0.0	-2.256	7.48×10^{19}
Se, $Bi_2O_7Sn_2$, Cu_3Se_2, Bi_2O_3	-0.865	-0.62	-1.435	0.0	-3.026	7.5×10^{19}
Cu_2O, $Bi_2O_7Sn_2$, Cu_2Se, Cu_3Se_2	-0.285	-0.318	-1.864	-0.453	-2.104	1.13×10^{19}
O_2Sn, $Bi_2O_7Sn_2$, Cu_2Se, Cu_3Se_2	-0.104	-0.318	-2.045	-0.453	-1.652	1.13×10^{19}
Cu_2O, $Bi_2O_7Sn_2$, Cu_3Se_2, Bi_2O_3	-0.603	-0.445	-1.61	-0.262	-2.676	2.61×10^{19}
Bi, Cu_2O, $Bi_2O_7Sn_2$, Bi_2O_3	0.0	-0.244	-2.012	-0.664	-1.873	5.61×10^{18}
Bi, O_2Sn, $Bi_2O_7Sn_2$, Cu_2Se	0.0	-0.283	-2.114	-0.522	-1.513	8.61×10^{18}
Bi, Cu_2O, $Bi_2O_7Sn_2$, Cu_2Se	0.0	-0.223	-2.054	-0.643	-1.724	5.11×10^{18}
Bi, O_2Sn, Cu_2Se, Cu_3Se_2	0.0	-0.318	-2.149	-0.453	-1.444	1.11×10^{19}
Bi, O_2Sn, Cu_3Se_2, Bi_2Se_3	0.0	-0.452	-2.216	-0.252	-1.31	2.34×10^{19}
Bi, Bi_2O_2Se, $Bi_2O_7Sn_2$, Bi_2O_3	0.0	-0.507	-2.012	-0.402	-1.873	3.45×10^{19}
Bi, Bi_2O_2Se, $Bi_2O_7Sn_2$, Bi_2Se_3	0.0	-0.582	-2.087	-0.252	-1.61	5.39×10^{19}
Bi, O_2Sn, $Bi_2O_7Sn_2$, Bi_2Se_3	0.0	-0.554	-2.114	-0.252	-1.513	4.52×10^{19}

Table S16: Chemical potentials $\Delta\mu_{\mathrm{i}}$ (in eV) in all phase regions of the quinary Bi-Cu-Se-O-Sn phase space that are in equilibrium with BiCuSeO. The corresponding charge carrier concentration in each phase region, as determined by charge neutrality at the typical synthesis temperature of 973 K, is listed.

Phase Equilibriua of Pb-Doped BiCuSeO

Equilibrium Phases	$\Delta\mu_{\mathrm{Bi}}$	$\Delta\mu_{\mathrm{Cu}}$	$\Delta\mu_{\mathrm{O}}$	$\Delta\mu_{\mathrm{Pb}}$	$\Delta\mu_{\mathrm{Se}}$	$p-n$ (cm^{-3})
Se, PbSe, Cu_3Se_2, Bi_2Se_3	-0.378	-0.62	-1.923	-0.942	0.0	8.28×10^{19}
Se, PbSe, Bi_2O_2Se, Bi_2O_3	-0.602	-0.708	-1.61	-0.942	0.0	1.92×10^{20}
Se, PbSe, Bi_2O_2Se, Bi_2Se_3	-0.378	-0.708	-1.835	-0.942	0.0	1.3×10^{20}
Se, PbSe, Cu_3Se_2, O_5Pb_3Se	-0.772	-0.62	-1.528	-0.942	0.0	4×10^{20}
Se, O_3PbSe, Cu_3Se_2, O_5Pb_3Se	-0.773	-0.62	-1.527	-0.943	0.0	4×10^{20}
Se, O_3PbSe, Cu_3Se_2, Bi_2O_3	-0.865	-0.62	-1.435	-1.22	0.0	1.54×10^{20}
Se, O_3PbSe, Bi_2O_3, O_5Pb_3Se	-0.727	-0.666	-1.527	-0.943	0.0	3.17×10^{20}
Se, PbSe, Bi_2O_3, O_5Pb_3Se	-0.726	-0.667	-1.528	-0.942	0.0	3.17×10^{20}
Bi, PbSe, Bi_2O_2Se, Bi_2Se_3	0.0	-0.582	-2.087	-0.69	-0.252	5.62×10^{19}
Bi, Cu_2Se, Cu_2O_2Pb, OPb	0.0	-0.228	-2.059	-0.335	-0.632	6.01×10^{19}
Bi, PbSe, Cu_2Se, OPb	0.0	-0.237	-2.068	-0.326	-0.616	6.59×10^{19}
Bi, Cu_2Se, Cu_2O, Cu_2O_2Pb	0.0	-0.223	-2.054	-0.356	-0.643	5.31×10^{19}
Bi, Cu_2O_2Pb, Bi_2O_3, OPb	0.0	-0.252	-2.012	-0.382	-0.656	4.6×10^{19}
Bi, Cu_2O, Cu_2O_2Pb, Bi_2O_3	0.0	-0.244	-2.012	-0.398	-0.664	4.18×10^{19}
Bi, PbSe, Bi_2O_3, OPb	0.0	-0.349	-2.012	-0.382	-0.56	6.32×10^{19}
Bi, PbSe, Bi_2O_2Se, Bi_2O_3	0.0	-0.507	-2.012	-0.54	-0.402	5.11×10^{19}
Bi, PbSe, Cu_3Se_2, Bi_2Se_3	0.0	-0.452	-2.216	-0.69	-0.252	2.74×10^{19}
Bi, PbSe, Cu_2Se, Cu_3Se_2	0.0	-0.318	-2.149	-0.489	-0.453	4.58×10^{19}
Cu_2O, Cu_2O_2Pb, Cu_3Se_2, Bi_2O_3	-0.603	-0.445	-1.61	-0.8	-0.262	2.94×10^{20}
Cu_2O_2Pb, Cu_3Se_2, Bi_2O_3, OPb	-0.627	-0.461	-1.594	-0.8	-0.238	3.42×10^{20}
PbSe, Cu_3Se_2, O_5Pb_3Se, OPb	-0.679	-0.536	-1.579	-0.815	-0.127	4.58×10^{20}
Cu_3Se_2, Bi_2O_3, O_5Pb_3Se, OPb	-0.688	-0.502	-1.553	-0.841	-0.178	4.03×10^{20}
O_3PbSe, Cu_3Se_2, Bi_2O_3, O_5Pb_3Se	-0.786	-0.567	-1.488	-0.983	-0.079	3.36×10^{20}
PbSe, Bi_2O_3, O_5Pb_3Se, OPb	-0.649	-0.565	-1.579	-0.815	-0.127	3.91×10^{20}
PbSe, Cu_2Se, Cu_3Se_2, OPb	-0.244	-0.318	-1.905	-0.489	-0.453	1.56×10^{20}
Cu_2Se, Cu_2O_2Pb, Cu_3Se_2, OPb	-0.269	-0.318	-1.88	-0.514	-0.453	1.56×10^{20}
Cu_2Se, Cu_2O, Cu_2O_2Pb, Cu_3Se_2	-0.285	-0.318	-1.864	-0.546	-0.453	1.46×10^{20}

Table S17: Chemical potentials $\Delta\mu_{\mathrm{i}}$ (in eV) in all phase regions of the quinary Bi-Cu-Se-O-Pb phase space that are in equilibrium with BiCuSeO. The corresponding charge carrier concentration in each phase region, as determined by charge neutrality at the typical synthesis temperature of 973 K, is listed.

Phase Equilibriua of Sc-Doped BiCuSeO

Equilibrium Phases	$\Delta\mu_{\mathrm{Bi}}$	$\Delta\mu_{\mathrm{Cu}}$	$\Delta\mu_{\mathrm{O}}$	$\Delta\mu_{\mathrm{Sc}}$	$\Delta\mu_{\mathrm{Se}}$	$p-n$ (cm^{-3})
Se, O_3Sc_2, Cu_3Se_2, Bi_2Se_3	-0.378	-0.62	-1.923	-6.969	0.0	7.36×10^{19}
Se, O_3Sc_2, Bi_2O_2Se, Bi_2O_3	-0.602	-0.708	-1.61	-7.437	0.0	1.26×10^{20}
Se, O_3Sc_2, Bi_2O_2Se, Bi_2Se_3	-0.378	-0.708	-1.835	-7.1	0.0	1.25×10^{20}
Se, O_3Sc_2, Cu_3Se_2, Bi_2O_3	-0.865	-0.62	-1.435	-7.7	0.0	7.5×10^{19}
Bi, O_3Sc_2, Bi_2O_2Se, Bi_2Se_3	0.0	-0.582	-2.087	-6.723	-0.252	5.39×10^{19}
Bi, Cu_2Se, Cu_2O, CuO_2Sc	0.0	-0.223	-2.054	-6.817	-0.643	5.11×10^{18}
Bi, O_3Sc_2, Cu_2Se, CuO_2Sc	0.0	-0.253	-2.084	-6.726	-0.582	6.72×10^{18}
Bi, O_3Sc_2, CuO_2Sc, Bi_2O_3	0.0	-0.29	-2.012	-6.835	-0.619	7.98×10^{18}
Bi, Cu_2O, CuO_2Sc, Bi_2O_3	0.0	-0.244	-2.012	-6.881	-0.664	5.61×10^{18}
Bi, O_3Sc_2, Bi_2O_2Se, Bi_2O_3	0.0	-0.507	-2.012	-6.835	-0.402	3.45×10^{19}
Bi, O_3Sc_2, Cu_3Se_2, Bi_2Se_3	0.0	-0.452	-2.216	-6.528	-0.252	2.34×10^{19}
Bi, O_3Sc_2, Cu_2Se, Cu_3Se_2	0.0	-0.318	-2.149	-6.629	-0.453	1.1×10^{19}
O_3Sc_2, Cu_2Se, CuO_2Sc, Cu_3Se_2	-0.194	-0.318	-1.955	-6.92	-0.453	1.13×10^{19}
Cu_2Se, Cu_2O, CuO_2Sc, Cu_3Se_2	-0.285	-0.318	-1.864	-7.102	-0.453	1.13×10^{19}
O_3Sc_2, CuO_2Sc, Cu_3Se_2, Bi_2O_3	-0.739	-0.536	-1.519	-7.574	-0.126	4.54×10^{19}
Cu_2O, CuO_2Sc, Cu_3Se_2, Bi_2O_3	-0.603	-0.445	-1.61	-7.483	-0.262	2.61×10^{19}

Table S18: Chemical potentials $\Delta\mu_{\mathrm{i}}$ (in eV) in all phase regions of the quinary Bi-Cu-Se-O-Sc phase space that are in equilibrium with BiCuSeO. The corresponding charge carrier concentration in each phase region, as determined by charge neutrality at the typical synthesis temperature of 973 K, is listed.

Phase Equilibriua of Y-Doped BiCuSeO

Equilibrium Phases	$\Delta\mu_{\mathrm{Bi}}$	$\Delta\mu_{\mathrm{Cu}}$	$\Delta\mu_{\mathrm{O}}$	$\Delta\mu_{\mathrm{Se}}$	$\Delta\mu_{\mathrm{Y}}$	$p-n$ (cm^{-3})
Bi, Bi_2O_2Se, Bi_2Se_3, O_3Y_2	0.0	-0.582	-2.087	-0.252	-6.748	5.31e+19
Bi, Cu_2O, Bi_2O_3, O_3Y_2	0.0	-0.244	-2.012	-0.664	-6.86	5.59e+18
Bi, Cu_2Se, Cu_2O, O_3Y_2	0.0	-0.223	-2.054	-0.643	-6.796	5.08e+18
Bi, Bi_2O_2Se, Bi_2O_3, O_3Y_2	0.0	-0.507	-2.012	-0.402	-6.86	3.44e+19
Bi, Cu_3Se_2, Bi_2Se_3, O_3Y_2	0.0	-0.452	-2.216	-0.252	-6.553	2.04e+19
Bi, Cu_2Se, Cu_3Se_2, O_3Y_2	0.0	-0.318	-2.149	-0.453	-6.654	1.05e+19
Cu_2Se, Cu_2O, Cu_3Se_2, O_3Y_2	-0.285	-0.318	-1.864	-0.453	-7.082	1.12e+19
Cu_2O, Cu_3Se_2, Bi_2O_3, O_3Y_2	-0.603	-0.445	-1.61	-0.262	-7.463	2.59e+19
Se, Cu_3Se_2, Bi_2O_3, O_3Y_2	-0.865	-0.62	-1.435	0.0	-7.725	7.46e+19
Se, Bi_2O_2Se, Bi_2Se_3, O_3Y_2	-0.378	-0.708	-1.835	0.0	-7.125	1.22e+20
Se, Bi_2O_2Se, Bi_2O_3, O_3Y_2	-0.602	-0.708	-1.61	0.0	-7.462	1.25e+20
Se, Cu_3Se_2, Bi_2Se_3, O_3Y_2	-0.378	-0.62	-1.923	0.0	-6.994	6.67e+19

Table S19: Chemical potentials $\Delta\mu_{\mathrm{i}}$ (in eV) in all phase regions of the quinary Bi-Cu-Se-O-Y phase space that are in equilibrium with BiCuSeO. The corresponding charge carrier concentration in each phase region, as determined by charge neutrality at the typical synthesis temperature of 973 K, is listed.

Phase Equilibriua of Ti-Doped BiCuSeO

Equilibrium Phases	$\Delta\mu_{\mathrm{Bi}}$	$\Delta\mu_{\mathrm{Cu}}$	$\Delta\mu_{\mathrm{O}}$	$\Delta\mu_{\mathrm{Se}}$	$\Delta\mu_{\mathrm{Ti}}$	$p-n$ (cm^{-3})
Bi, Bi_2O_2Se, $Bi_2O_7Ti_2$, Bi_2Se_3	0.0	-0.582	-2.087	-0.252	-5.733	5.39×10^{19}
Bi, $Bi_2O_7Ti_2$, O_2Ti, Bi_2Se_3	0.0	-0.567	-2.101	-0.252	-5.683	4.91×10^{19}
Bi, Bi_2O_2Se, $Bi_2O_7Ti_2$, Bi_2O_3	0.0	-0.507	-2.012	-0.402	-5.996	3.45×10^{19}
Bi, Cu_2Se, Cu_2O, $Bi_2O_7Ti_2$	0.0	-0.223	-2.054	-0.643	-5.847	5.11×10^{18}
Bi, Cu_2Se, $Bi_2O_7Ti_2$, O_2Ti	0.0	-0.27	-2.101	-0.549	-5.683	7.74×10^{18}
Bi, Cu_2O, $Bi_2O_7Ti_2$, Bi_2O_3	0.0	-0.244	-2.012	-0.664	-5.996	5.61×10^{18}
Bi, Cu_3Se_2, O_2Ti, Bi_2Se_3	0.0	-0.452	-2.216	-0.252	-5.453	2.34×10^{19}
Bi, Cu_2Se, Cu_3Se_2, O_2Ti	0.0	-0.318	-2.149	-0.453	-5.587	1.1×10^{19}
Cu_2Se, Cu_2O, $Bi_2O_7Ti_2$, Cu_3Se_2	-0.285	-0.318	-1.864	-0.453	-6.227	1.13×10^{19}
Cu_2Se, $Bi_2O_7Ti_2$, Cu_3Se_2, O_2Ti	-0.144	-0.318	-2.005	-0.453	-5.875	1.13×10^{19}
Cu_2O, $Bi_2O_7Ti_2$, Cu_3Se_2, Bi_2O_3	-0.603	-0.445	-1.61	-0.262	-6.799	2.61×10^{19}
Se, $Bi_2O_7Ti_2$, Cu_3Se_2, Bi_2O_3	-0.865	-0.62	-1.435	0.0	-7.149	7.5×10^{19}
Se, $Bi_2O_7Ti_2$, Cu_3Se_2, O_2Ti	-0.597	-0.62	-1.703	0.0	-6.479	7.48×10^{19}
Se, Bi_2O_2Se, $Bi_2O_7Ti_2$, Bi_2Se_3	-0.378	-0.708	-1.835	0.0	-6.237	1.25×10^{20}
Se, $Bi_2O_7Ti_2$, O_2Ti, Bi_2Se_3	-0.378	-0.693	-1.849	0.0	-6.186	1.14×10^{20}
Se, Bi_2O_2Se, $Bi_2O_7Ti_2$, Bi_2O_3	-0.602	-0.708	-1.61	0.0	-6.799	1.26×10^{20}
Se, Cu_3Se_2, O_2Ti, Bi_2Se_3	-0.378	-0.62	-1.923	0.0	-6.04	7.36×10^{19}

Table S20: Chemical potentials $\Delta\mu_{\mathrm{i}}$ (in eV) in all phase regions of the quinary Bi-Cu-Se-O-Ti phase space that are in equilibrium with BiCuSeO. The corresponding charge carrier concentration in each phase region, as determined by charge neutrality at the typical synthesis temperature of 973 K, is listed.

Phase Equilibriua of Zr-Doped BiCuSeO

Equilibrium Phases	$\Delta\mu_{\mathrm{Bi}}$	$\Delta\mu_{\mathrm{Cu}}$	$\Delta\mu_{\mathrm{O}}$	$\Delta\mu_{\mathrm{Se}}$	$\Delta\mu_{\mathrm{Zr}}$	$p-n$ (cm^{-3})
Bi, Bi_2O_2Se, O_2Zr, Bi_2Se_3	0.0	-0.582	-2.087	-0.252	-7.229	5.39×10^{19}
Bi, Cu_2Se, Cu_2O, O_2Zr	0.0	-0.223	-2.054	-0.643	-7.294	5.11×10^{18}
Bi, Cu_2O, O_2Zr, Bi_2O_3	0.0	-0.244	-2.012	-0.664	-7.379	5.61×10^{18}
Bi, Bi_2O_2Se, O_2Zr, Bi_2O_3	0.0	-0.507	-2.012	-0.402	-7.379	3.45×10^{19}
Bi, O_2Zr, Cu_3Se_2, Bi_2Se_3	0.0	-0.452	-2.216	-0.252	-6.97	2.34×10^{19}
Bi, Cu_2Se, O_2Zr, Cu_3Se_2	0.0	-0.318	-2.149	-0.453	-7.104	1.1×10^{19}
Cu_2O, O_2Zr, Cu_3Se_2, Bi_2O_3	-0.603	-0.445	-1.61	-0.262	-8.182	2.61×10^{19}
Cu_2Se, Cu_2O, O_2Zr, Cu_3Se_2	-0.285	-0.318	-1.864	-0.453	-7.674	1.13×10^{19}
Se, O_2Zr, Cu_3Se_2, Bi_2O_3	-0.865	-0.62	-1.435	0.0	-8.532	7.5×10^{19}
Se, Bi_2O_2Se, O_2Zr, Bi_2Se_3	-0.378	-0.708	-1.835	0.0	-7.732	1.25×10^{20}
Se, Bi_2O_2Se, O_2Zr, Bi_2O_3	-0.602	-0.708	-1.61	0.0	-8.182	1.26×10^{20}
Se, O_2Zr, Cu_3Se_2, Bi_2Se_3	-0.378	-0.62	-1.923	0.0	-7.557	7.36×10^{19}

Table S21: Chemical potentials $\Delta\mu_{\mathrm{i}}$ (in eV) in all phase regions of the quinary Bi-Cu-Se-O-Zr phase space that are in equilibrium with BiCuSeO. The corresponding charge carrier concentration in each phase region, as determined by charge neutrality at the typical synthesis temperature of 973 K, is listed.

Phase Equilibriua of Hf-Doped BiCuSeO

Equilibrium Phases	$\Delta\mu_{\mathrm{Bi}}$	$\Delta\mu_{\mathrm{Cu}}$	$\Delta\mu_{\mathrm{Hf}}$	$\Delta\mu_{\mathrm{O}}$	$\Delta\mu_{\mathrm{Se}}$	$p-n$ (cm^{-3})
Se, HfO_2, Cu_3Se_2, Bi_2Se_3	-0.378	-0.62	-8.0	-1.923	0.0	7.36×10^{19}
Se, Bi_2O_2Se, HfO_2, $Bi_8Hf_8O_{28}$	-0.517	-0.708	-8.454	-1.695	0.0	1.25×10^{20}
Se, Bi_2O_2Se, Bi_2O_3, $Bi_8Hf_8O_{28}$	-0.603	-0.708	-8.668	-1.61	0.0	1.26×10^{20}
Se, Bi_2O_2Se, HfO_2, Bi_2Se_3	-0.378	-0.708	-8.175	-1.835	0.0	1.25×10^{20}
Se, HfO_2, Cu_3Se_2, $Bi_8Hf_8O_{28}$	-0.78	-0.62	-8.805	-1.52	0.0	7.48×10^{19}
Se, Cu_3Se_2, Bi_2O_3, $Bi_8Hf_8O_{28}$	-0.865	-0.62	-9.018	-1.435	0.0	7.48×10^{19}
Bi, Bi_2O_2Se, HfO_2, Bi_2Se_3	0.0	-0.582	-7.672	-2.087	-0.252	5.4×10^{19}
Bi, Cu_2Se, Cu_2O, HfO_2	0.0	-0.223	-7.737	-2.054	-0.643	5.11×10^{18}
Bi, Cu_2O, HfO_2, $Bi_8Hf_8O_{28}$	0.0	-0.23	-7.765	-2.04	-0.65	5.29×10^{18}
Bi, Cu_2O, Bi_2O_3, $Bi_8Hf_8O_{28}$	0.0	-0.244	-7.864	-2.012	-0.664	5.61×10^{18}
Bi, Bi_2O_2Se, Bi_2O_3, $Bi_8Hf_8O_{28}$	0.0	-0.507	-7.864	-2.012	-0.402	3.44×10^{19}
Bi, Bi_2O_2Se, HfO_2, $Bi_8Hf_8O_{28}$	0.0	-0.535	-7.765	-2.04	-0.345	4.14×10^{19}
Bi, HfO_2, Cu_3Se_2, Bi_2Se_3	0.0	-0.452	-7.413	-2.216	-0.252	2.33×10^{19}
Bi, Cu_2Se, HfO_2, Cu_3Se_2	0.0	-0.318	-7.547	-2.149	-0.453	1.1×10^{19}
Cu_2O, Cu_3Se_2, Bi_2O_3, $Bi_8Hf_8O_{28}$	-0.603	-0.445	-8.668	-1.61	-0.262	2.6×10^{19}
Cu_2O, HfO_2, Cu_3Se_2, $Bi_8Hf_8O_{28}$	-0.39	-0.36	-8.284	-1.78	-0.39	1.51×10^{19}
Cu_2Se, Cu_2O, HfO_2, Cu_3Se_2	-0.285	-0.318	-8.117	-1.864	-0.453	1.13×10^{19}

Table S22: Chemical potentials $\Delta\mu_{\mathrm{i}}$ (in eV) in all phase regions of the quinary Bi-Cu-Se-O-Hf phase space that are in equilibrium with BiCuSeO. The corresponding charge carrier concentration in each phase region, as determined by charge neutrality at the typical synthesis temperature of 973 K, is listed.

Phase Equilibria of F-Doped BiCuSeO

Equilibrium Phases	$\Delta\mu_{\mathrm{Bi}}$	$\Delta\mu_{\mathrm{Cu}}$	$\Delta\mu_{\mathrm{F}}$	$\Delta\mu_{\mathrm{O}}$	$\Delta\mu_{\mathrm{Se}}$	$p-n$ (cm^{-3})
Cu_2O, Cu_3Se_2, Bi_2O_3, BiFO	-0.632	-0.465	-3.449	-1.601	-0.25	2.62×10^{19}
Cu_3Se_2, $Bi_7F_{11}O_5$, Cu_2Se, BiFO	-0.263	-0.349	-3.507	-1.913	-0.423	8.12×10^{18}
Cu_2O, Cu_3Se_2, Cu_2Se, BiFO	-0.343	-0.349	-3.507	-1.832	-0.423	9.53×10^{18}
Bi, Cu_3Se_2, $Bi_7F_{11}O_5$, Cu_2Se	0.0	-0.349	-3.555	-2.176	-0.423	2.99×10^{18}
Bi, Cu_3Se_2, $Bi_7F_{11}O_5$, Bi_2Se_3	0.0	-0.46	-3.53	-2.231	-0.256	3.82×10^{18}
Bi, $Bi_7F_{11}O_5$, Bi_2O_2Se, BiFO	0.0	-0.583	-3.595	-2.088	-0.277	2.61×10^{19}
Bi, Bi_2O_3, Bi_2O_2Se, BiFO	0.0	-0.518	-3.66	-2.023	-0.408	2.77×10^{19}
Bi, $Bi_7F_{11}O_5$, Cu_2Se, BiFO	0.0	-0.262	-3.595	-2.088	-0.598	2.93×10^{18}
Bi, Cu_2O, Cu_2Se, BiFO	0.0	-0.235	-3.621	-2.061	-0.652	2.61×10^{18}
Bi, Cu_2O, Bi_2O_3, BiFO	0.0	-0.254	-3.66	-2.023	-0.671	3.59×10^{18}
Bi, $Bi_7F_{11}O_5$, Bi_2O_2Se, Bi_2Se_3	0.0	-0.593	-3.59	-2.098	-0.256	2.59×10^{19}
Se, Cu_3Se_2, $Bi_7F_{11}O_5$, BiFO	-0.686	-0.631	-3.366	-1.631	0.0	7×10^{19}
Se, Cu_3Se_2, Bi_2O_3, BiFO	-0.882	-0.631	-3.366	-1.435	0.0	7.77×10^{19}
Se, $Bi_7F_{11}O_5$, Bi_2O_2Se, Bi_2Se_3	-0.385	-0.722	-3.462	-1.842	0.0	9.44×10^{19}
Se, Bi_2O_3, Bi_2O_2Se, BiFO	-0.611	-0.722	-3.456	-1.615	0.0	1.31×10^{20}
Se, $Bi_7F_{11}O_5$, Bi_2O_2Se, BiFO	-0.415	-0.722	-3.456	-1.811	0.0	1.01×10^{20}
Se, Cu_3Se_2, $Bi_7F_{11}O_5$, Bi_2Se_3	-0.385	-0.631	-3.421	-1.932	0.0	3.23×10^{19}

Table S23: Chemical potentials $\Delta\mu_{\mathrm{i}}$ (in eV) in all phase regions of the quinary Bi-Cu-Se-O-F phase space that are in equilibrium with BiCuSeO. The corresponding charge carrier concentration in each phase region, as determined by charge neutrality at the typical synthesis temperature of 973 K, is listed.

Phase Equilibria of Cl-Doped BiCuSeO

Equilibrium Phases	$\Delta\mu_{Bi}$	$\Delta\mu_{Cl}$	$\Delta\mu_{Cu}$	$\Delta\mu_{O}$	$\Delta\mu_{Se}$	$p-n$ (cm^{-3})
Se, BiClO, Cu_3Se_2, Bi_2Se_3	-0.378	-1.43	-0.62	-1.923	0.0	3.32×10^{19}
Se, Bi_2O_2Se, Bi_2O_3, $Bi_{48}Cl_{20}O_{62}$	-0.603	-1.627	-0.708	-1.61	0.0	1.05×10^{20}
Se, BiClO, Bi_2O_2Se, $Bi_{48}Cl_{20}O_{62}$	-0.446	-1.518	-0.708	-1.767	0.0	7.95×10^{19}
Se, BiClO, Bi_2O_2Se, Bi_2Se_3	-0.378	-1.518	-0.708	-1.835	0.0	7.92×10^{19}
Se, BiClO, Cu_3Se_2, $Bi_{48}Cl_{20}O_{62}$	-0.708	-1.43	-0.62	-1.592	0.0	3.34×10^{19}
Se, Cu_3Se_2, Bi_2O_3, $Bi_{48}Cl_{20}O_{62}$	-0.865	-1.54	-0.62	-1.435	0.0	5.15×10^{19}
Bi, BiClO, Bi_2O_2Se, Bi_2Se_3	0.0	-1.643	-0.582	-2.087	-0.252	2.18×10^{19}
Bi, BiClO, Bi_2O_2Se, $Bi_{48}Cl_{20}O_{62}$	0.0	-1.666	-0.559	-2.064	-0.297	1.71×10^{19}
Bi, Bi_2O_2Se, Bi_2O_3, $Bi_{48}Cl_{20}O_{62}$	0.0	-1.828	-0.507	-2.012	-0.402	1.66×10^{19}
Bi, Cu_2Se, Cu_2O, $Bi_{48}Cl_{20}O_{62}$	0.0	-1.697	-0.223	-2.054	-0.643	-2.32×10^{18}
Bi, Cu_2Se, BiClO, $Bi_{48}Cl_{20}O_{62}$	0.0	-1.666	-0.233	-2.064	-0.623	-2.35×10^{18}
Bi, Cu_2O, Bi_2O_3, $Bi_{48}Cl_{20}O_{62}$	0.0	-1.828	-0.244	-2.012	-0.664	-4.58×10^{17}
Bi, BiClO, Cu_3Se_2, Bi_2Se_3	0.0	-1.514	-0.452	-2.216	-0.252	4.83×10^{18}
Bi, Cu_2Se, BiClO, Cu_3Se_2	0.0	-1.581	-0.318	-2.149	-0.453	9.94×10^{14}
Cu_2O, Cu_3Se_2, Bi_2O_3, $Bi_{48}Cl_{20}O_{62}$	-0.603	-1.627	-0.445	-1.61	-0.262	8.51×10^{18}
Cu_2Se, BiClO, Cu_3Se_2, $Bi_{48}Cl_{20}O_{62}$	-0.255	-1.581	-0.318	-1.894	-0.453	3.5×10^{16}
Cu_2Se, Cu_2O, Cu_3Se_2, $Bi_{48}Cl_{20}O_{62}$	-0.285	-1.602	-0.318	-1.864	-0.453	3.02×10^{17}

Table S24: Chemical potentials $\Delta\mu_i$ (in eV) in all phase regions of the quinary Bi-Cu-Se-O-Cl phase space that are in equilibrium with BiCuSeO. The corresponding charge carrier concentration in each phase region, as determined by charge neutrality at the typical synthesis temperature of 973 K, is listed.

Phase Equilibria of Br-Doped BiCuSeO

Equilibrium Phases	$\Delta\mu_{Bi}$	$\Delta\mu_{Br}$	$\Delta\mu_{Cu}$	$\Delta\mu_{O}$	$\Delta\mu_{Se}$	$p-n$ (cm^{-3})
$Bi_4Br_2O_5$, Cu_2O, Cu_3Se_2, Bi_2O_3	-0.603	-1.082	-0.445	-1.61	-0.262	1.02×10^{19}
$Bi_4Br_2O_5$, Cu_3Se_2, Bi_2O_3, $Bi_6Br_2O_{14}Se_3$	-0.833	-1.006	-0.599	-1.456	-0.032	4.75×10^{19}
$Bi_4Br_2O_5$, Cu_2Se, Cu_3Se_2, BiBrO	-0.152	-1.016	-0.318	-1.997	-0.453	2.06×10^{17}
$Bi_4Br_2O_5$, Cu_2O, Cu_2Se, Cu_3Se_2	-0.285	-1.082	-0.318	-1.864	-0.453	1.07×10^{18}
Bi, Cu_2Se, Cu_3Se_2, BiBrO	0.0	-1.016	-0.318	-2.149	-0.453	1.92×10^{17}
Bi, Cu_3Se_2, BiBrO, Bi_2Se_3	0.0	-0.949	-0.452	-2.216	-0.252	5.31×10^{18}
Bi, $Bi_4Br_2O_5$, Bi_2O_2Se, Bi_2O_3	0.0	-1.283	-0.507	-2.012	-0.402	1.94×10^{19}
Bi, $Bi_4Br_2O_5$, Bi_2O_2Se, Bi_2Se_3	0.0	-1.096	-0.582	-2.087	-0.252	2.57×10^{19}
Bi, $Bi_4Br_2O_5$, BiBrO, Bi_2Se_3	0.0	-1.067	-0.57	-2.098	-0.252	2.08×10^{19}
Bi, $Bi_4Br_2O_5$, Cu_2O, Bi_2O_3	0.0	-1.283	-0.244	-2.012	-0.664	-2.62×10^{16}
Bi, $Bi_4Br_2O_5$, Cu_2O, Cu_2Se	0.0	-1.177	-0.223	-2.054	-0.643	-1.37×10^{18}
Bi, $Bi_4Br_2O_5$, Cu_2Se, BiBrO	0.0	-1.067	-0.267	-2.098	-0.554	-1.07×10^{18}
Se, $Bi_4Br_2O_5$, Bi_2O_3, $Bi_6Br_2O_{14}Se_3$	-0.809	-1.014	-0.639	-1.472	0.0	6.63×10^{19}
Se, Cu_3Se_2, Bi_2O_3, $Bi_6Br_2O_{14}Se_3$	-0.865	-1.108	-0.62	-1.435	0.0	6.84×10^{19}
Se, $Bi_4Br_2O_5$, Cu_3Se_2, BiBrO	-0.605	-0.865	-0.62	-1.695	0.0	3.58×10^{19}
Se, $Bi_4Br_2O_5$, Cu_3Se_2, $Bi_6Br_2O_{14}Se_3$	-0.833	-0.979	-0.62	-1.467	0.0	5.45×10^{19}
Se, $Bi_4Br_2O_5$, BiBrO, Bi_2Se_3	-0.378	-0.941	-0.696	-1.847	0.0	7.51×10^{19}
Se, $Bi_4Br_2O_5$, Bi_2O_2Se, Bi_2Se_3	-0.378	-0.97	-0.708	-1.835	0.0	8.8×10^{19}
Se, $Bi_4Br_2O_5$, Bi_2O_2Se, Bi_2O_3	-0.603	-1.083	-0.708	-1.61	0.0	1.11×10^{20}
Se, Cu_3Se_2, BiBrO, Bi_2Se_3	-0.378	-0.865	-0.62	-1.923	0.0	3.57×10^{19}

Table S25: Chemical potentials $\Delta\mu_i$ (in eV) in all phase regions of the quinary Bi-Cu-Se-O-Br phase space that are in equilibrium with BiCuSeO. The corresponding charge carrier concentration in each phase region, as determined by charge neutrality at the typical synthesis temperature of 973 K, is listed.

Phase Equilibria of I-Doped BiCuSeO

Equilibrium Phases	$\Delta\mu_{\mathrm{Bi}}$	$\Delta\mu_{\mathrm{Cu}}$	$\Delta\mu_{\mathrm{I}}$	$\Delta\mu_{\mathrm{O}}$	$\Delta\mu_{\mathrm{Se}}$	$p-n$ (cm^{-3})
Se, $Bi_4I_2O_5$, Bi_2O_2Se, Bi_2O_3	-0.602	-0.708	-0.547	-1.61	0.0	1.24×10^{20}
Se, $Bi_4I_2O_5$, Bi_2O_2Se, Bi_2Se_3	-0.378	-0.708	-0.435	-1.835	0.0	1.18×10^{20}
Se, BiIO, $Bi_4I_2O_5$, Bi_2Se_3	-0.378	-0.685	-0.379	-1.857	0.0	9.84×10^{19}
Se, BiIO, Cu_3Se_2, Bi_2Se_3	-0.378	-0.62	-0.314	-1.923	0.0	6.1×10^{19}
Se, BiIO, $Bi_4I_2O_5$, Cu_3Se_2	-0.573	-0.62	-0.314	-1.727	0.0	6.16×10^{19}
Se, $Bi_4I_2O_5$, Cu_3Se_2, Bi_2O_3	-0.865	-0.62	-0.46	-1.435	0.0	7.2×10^{19}
Bi, BiIO, CuI, Bi_2Se_3	0.0	-0.455	-0.401	-2.213	-0.252	1.33×10^{19}
Bi, BiIO, $Bi_4I_2O_5$, Bi_2Se_3	0.0	-0.559	-0.505	-2.109	-0.252	3.57×10^{19}
Bi, $Bi_4I_2O_5$, Bi_2O_2Se, Bi_2Se_3	0.0	-0.582	-0.561	-2.087	-0.252	4.6×10^{19}
Bi, Cu_2O, $Bi_4I_2O_5$, Bi_2O_3	0.0	-0.244	-0.748	-2.012	-0.664	2.41×10^{18}
Bi, $Bi_4I_2O_5$, Bi_2O_2Se, Bi_2O_3	0.0	-0.507	-0.748	-2.012	-0.402	3.1×10^{19}
Bi, BiIO, $Bi_4I_2O_5$, CuI	0.0	-0.351	-0.505	-2.109	-0.46	4.14×10^{18}
Bi, Cu_2Se, Cu_2O, $Bi_4I_2O_5$	0.0	-0.223	-0.642	-2.054	-0.643	9.13×10^{17}
Bi, Cu_2Se, $Bi_4I_2O_5$, CuI	0.0	-0.229	-0.627	-2.06	-0.63	9.66×10^{17}
Bi, Cu_3Se_2, CuI, Bi_2Se_3	0.0	-0.452	-0.404	-2.216	-0.252	1.32×10^{19}
Bi, Cu_2Se, Cu_3Se_2, CuI	0.0	-0.318	-0.538	-2.149	-0.453	4.2×10^{18}
BiIO, Cu_3Se_2, CuI, Bi_2Se_3	-0.027	-0.464	-0.392	-2.195	-0.234	1.47×10^{19}
BiIO, $Bi_4I_2O_5$, Cu_3Se_2, CuI	-0.339	-0.464	-0.392	-1.883	-0.234	1.5×10^{19}
Cu_2O, $Bi_4I_2O_5$, Cu_3Se_2, Bi_2O_3	-0.603	-0.445	-0.547	-1.61	-0.262	2.05×10^{19}
Cu_2Se, Cu_2O, $Bi_4I_2O_5$, Cu_3Se_2	-0.285	-0.318	-0.547	-1.864	-0.453	4.45×10^{18}
Cu_2Se, $Bi_4I_2O_5$, Cu_3Se_2, CuI	-0.266	-0.318	-0.538	-1.883	-0.453	4.22×10^{18}

Table S26: Chemical potentials $\Delta\mu_{\mathrm{i}}$ (in eV) in all phase regions of the quinary Bi-Cu-Se-O-I phase space that are in equilibrium with BiCuSeO. The corresponding charge carrier concentration in each phase region, as determined by charge neutrality at the typical synthesis temperature of 973 K, is listed.

References

(1) Hiramatsu, H.; Yanagi, H.; Kamiya, T.; Ueda, K.; Hirano, M.; Hosono, H. Crystal structures, optoelectronic properties, and electronic structures of layered oxychalcogenides MCuOCh (M= Bi, La; Ch= S, Se, Te): effects of electronic configurations of M^{3+} ions. *Chem. Mater.* **2008**, *20*, 326.

(2) Lany, S. Semiconductor thermochemistry in density functional calculations. *Phys. Rev. B* **2008**, *78*, 245207.

(3) Stevanović, V.; Lany, S.; Zhang, X.; Zunger, A. Correcting density functional theory for accurate predictions of compound enthalpies of formation: Fitted elemental-phase reference energies. *Phys. Rev. B* **2012**, *85*, 115104.